Lidar Mapping Report

Acquisition, Processing, and Delivery of Airborne Lidar Elevation Data and Orthoimagery for the NE_PostSpringFlood_OrthoLidar_2019_D19 Project

USGS CONTRACT: G16PC00029

CONTRACTOR: Merrick-Surdex JV

TASK ORDER NUMBER: 140G0219F0170

TASK NAME:
NE_PostSpringFlood_OrthoLidar_2019_D19

GOVERNMENT POINT-OF-CONTACT (POC):
Michael Bradford, MS 665
U.S. Geological Survey – NGTOC
1400 Independence Road
Rolla, MO 65401
(573) 308-3629
mbradford@usgs.gov

Contract Project Manager:
Doug Jacoby
Merrick-Surdex Joint Venture, LLP (JV)
5970 Greenwood Plaza Blvd.
Greenwood Village, CO 80111
(303) 353-3903 (o)
(303) 521-6522 (c)
doug.jacoby@merrick.com

Contractor Job Number: J65220282

Submitted to:

USGS science for a changing world

Submitted by:

MERRICK SURDEX JOINT VENTURE

Table of Contents

Glossary of Terms

Term	Description
AGL	Above Ground Level
AGPS	Airborne Global Positioning System
ANPD	Aggregate Nominal Pulse Density
ANPS	Aggregate Nominal Pulse Spacing
ASPRS	American Society of Photogrammetry and Remote Sensing
AT	Aerial Triangulation
CD	Compact Disk
CMS	Certified Mapping Scientist
CORS	Continuous Operating Reference Station
CP	Certified Photogrammetrist
CVA	Consolidated Vertical Accuracy
DACS™	Digital Airborne Camera System
DEM	Digital Elevation Model
DFIRM	Digital Flood Insurance Rate Maps
DSM	Digital Surface Model
DTM	Digital Terrain Model
DVD	Digital Versatile Disk / Digital Video Disk
DXF	Data Exchange Format / Drawing Interchange
FIRM	Flood Insurance Rate Maps
FEMA	Federal Emergency Management
FGDC	Federal Geographic Data Committee
FVA	Fundamental Vertical Accuracy
FY	Fiscal Year
GIS	Geographic Information System
GISP	Geographic Information System Professional
GNSS	Global Navigation Satellite System
GPS	Global Positioning System
GSD	Ground Sample Distance
HARN	High Accuracy Reference Network
HDD	Hard Drive Disk
HPGN	High Precision Geodetic Network
IMU	Inertial Measurement Unit
INS	Inertial Navigation System
LAS	(or .las) – industry accepted LIDAR data exchange file format
LB	License Business
LS	Land Surveyor
LiDAR	(or Lidar) Light Detection And Ranging
MARS®	Merrick Advanced Remote Sensing
Merrick	Merrick & Company
MSL	Mean Sea Level
NAD	North American Datum
NDEP	National Digital Elevation Program
NGP	National Geospatial Program
NGS	National Geodetic Survey
NMAS	National Map Accuracy Standards
No.	Number
NPS	Nominal Point Spacing

NSRS	National Spatial Reference System
NSSDA	National Standard for Spatial Data
NVA	Non-vegetated Vertical Accuracy
OPUS	Online Positioning User Service
PDOP	Positional Dilution Of Precision
PLS	Professional Land Surveyor
PLSS	Public Land Survey System
ppsm	Points (or pulses) per square meter
PSM	Professional Surveyor and Mapper
QL1	Quality Level One
QL2	Quality Level Two
RLS	Registered Land Surveyor
RGB	Red, Green, Blue (i.e., three-band image)
RGBNIR	Red, Green, Blue, Near Infra-Red (i.e., four-band image)
RMSE	Root Mean Square Error
SBET	Smoothed Best Estimated Trajectory
SHA	Secured Hash Standard
SPCS	State Plane Coordinate System
SVA	Supplemental Vertical Accuracy
TIN	Triangular Irregular Network
USGS	United State Geological Survey
VVA	Vegetated Vertical Accuracy
XML	eXtensible Markup Language

Project Summary

The USGS awarded Merrick-Surdex Joint Venture, LLP (Merrick-Surdex JV) the NE_PostSpringFlood_OrthoLidar_2019_D19 (USGS Task Order Number 140G0219F0170) project as an emergency task order to support the Federal Emergency Management (FEMA) Risk Mapping, Assessment, and Planning (MAP) program with post-flood reclamation projects in the state of Nebraska by providing high resolution digital elevation lidar data and 4-band digital orthophotography. The project covers portions of 36 counties in Nebraska: Antelope, Boone, Boyd, Brown, Burt, Butler, Cass, Cedar, Colfax, Cuming, Dakota, Dixon, Dodge, Douglas, Greeley, Hamilton, Holt, Howard, Keya, Paha, Knox, Madison, Merrick, Nance, Nemaha, Otoe, Pierce, Platte, Polk, Richardson, Rock, Sarpy, Saunders, Stanton, Thurston, Washington, and Wayne totaling approximately 3,676 square miles. Lidar is being delivered for approximately 3,344 square miles. This is a result of removing approximately 332 square miles of all portions of Cass, Sarpy, Douglas, Washington, Nemaha, Otoe and Richardson counties due to high water conditions.

The lidar mapping requirements and deliverables meet Quality Level One (QL1) standards for final deliverables as outlined in the USGS-NGP Lidar Base Specifications, Techniques and Methods 11–B4, Version 1.3, February 2018 (TM11-B4) (http://pubs.usgs.gov/tm/11b4/pdf/tm11-B4.pdf). QL1 lidar specifications suggest a pulse density of greater than or equal to eight pulses per square meter (≥8ppsm) Aggregate Nominal Pulse Density (ANPD), and pulse spacing of less than or equal to thirty-five centimeters (≤0.35m) Aggregate Nominal Pulse Spacing (ANPS).

The vertical accuracy requirements of the lidar data meets or exceeds the following:

Absolute Vertical Accuracy

- ≤10cm RMSEz
- ≤19.6cm Non-vegetated Vertical Accuracy (NVA) at the 95% confidence level
- ≤30.0cm Vegetated Vertical Accuracy (VVA) at the 95% percentile

Relative Vertical Accuracy

- ≤6cm within individual swaths (smooth surface repeatability)
- ≤8cm $RMSD_Z$ within swath overlap (between adjacent swaths)

Project Spatial Reference

- Horizontal Datum – North American Datum of 1983 (NAD 83)
- Epoch – National Adjustment of 2011 (NA2011) (epoch 2010.00)
- Geoid – GEOID 12B
- Vertical Datum – North American Vertical Datum of 1988 (NAVD 88)
- Projection – Nebraska State Plane Coordinate System
- Units – U.S. Survey Feet

CONTACT INFORMATION

Questions regarding this report should be addressed to:

Doug Jacoby, CMS, GISP
Program Manager
Merrick & Company
5970 Greenwood Plaza Blvd.
Greenwood Village, CO 80111
T: +1 303-353-3903
Doug.jacoby@merrick.com

Project Report

The contents of this report summarize the methods used to calibrate and classify the lidar data as well as the results of these methods for the project NE_PostSpringFlood.

Lidar Flight Information

The acquisition area for the NE_PostSpringFlood project is delineated by the extent of the client approved Esri shapefile (*NE_Post_Flood_Tiles_10358_total_rev061919*). Merrick-Surdex JV acquired the QL1 lidar point cloud utilizing an Optech Galaxy lidar sensors. The Galaxy is a high performance lidar sensor capable of collecting large areas efficiently.

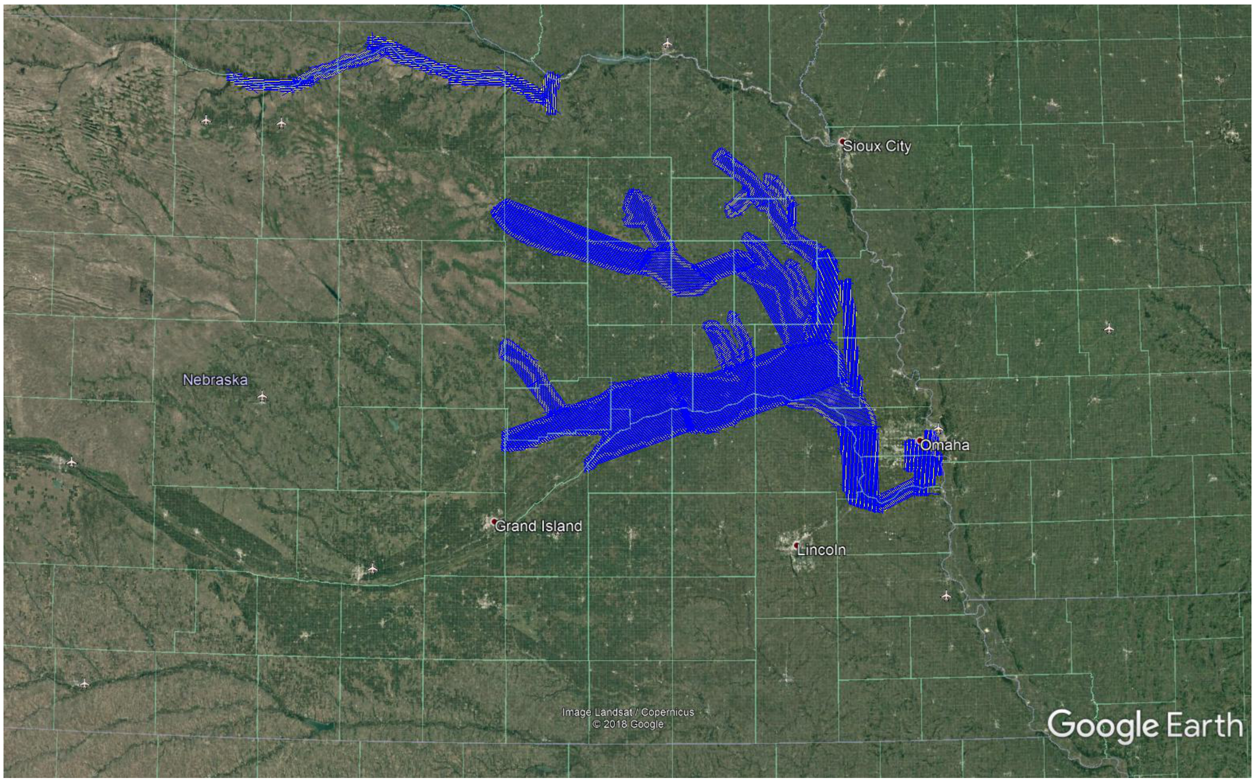

Aerial Mission(s)

Lidar acquisition was collected using a fixed wing aircraft and an Optech Galaxy lidar sensors staging from a variety of airports around the project area. Lidar data collection for the project was accomplished between May 25, 2019 and July 12, 2019. Each mission represents a lift of the aircraft and system from the ground, collects data, and lands again. Multiple lifts within a day are represented by Mission A, B, C, and D. The table below relates each mission to the date collected, the sensor and serial number used, and the actual average MSL in meters.

Mission(s)	Date	Sensor S/N	Actual Avg. MSL (m)
190525_A	May 25, 2019	5060314	1640
190525_B	May 25, 2019	5060314	1625
190526_A	May 26, 2019	5060314	1630

190526_B	May 26, 2019	5060314	1610
190526_A	May 26, 2019	5060382	1625
190530_A	May 30, 2019	5060314	1615
190530_B	May 30, 2019	5060314	1610
190530_C	May 30, 2019	5060314	1630
190531_A	May 31, 2019	5060314	1645
190531_B	May 31, 2019	5060314	1675
190531_C	May 31, 2019	5060314	1655
190531_A	May 31, 2019	5060382	1655
190531_A	May 31, 2019	5060407	1755
190531_B	May 31, 2019	5060407	1730
190531_C	May 31, 2019	5060407	1680
190531_D	May 31, 2019	5060407	1675
190601_A	June 1, 2019	5060380	2450
190601_A	June 1, 2019	5060314	1600
190601_B	June 1, 2019	5060314	1665
190601_C	June 1, 2019	5060314	1600
190601_A	June 1, 2019	5060407	1670
190601_B	June 1, 2019	5060407	1670
190602_A	June 2, 2019	5060380	2450
190602_A	June 2, 2019	5060314	1610
190602_B	June 2, 2019	5060314	1645
190602_A	June 2, 2019	5060382	1540
190602_A	June 2, 2019	5060407	1580
190602_B	June 2, 2019	5060407	1600
190603_A	June 3, 2019	5060314	1575
190603_A	June 3, 2019	5060407	1570
190604_A	June 4, 2019	5060380	2080
190604_A	June 4, 2019	5060314	1555
190604_B	June 4, 2019	5060314	1690
190604_C	June 4, 2019	5060382	1615
190604_D	June 4, 2019	5060382	1615
190604_A	June 4, 2019	5060407	1585
190604_B	June 4, 2019	5060407	1710
190604_C	June 4, 2019	5060407	1610
190604_D	June 4, 2019	5060407	1630
190605_A	June 5, 2019	5060380	2150
190605_A	June 5, 2019	5060314	1530
190605_A	June 5, 2019	5060382	1550
190605_B	June 5, 2019	5060382	1540
190605_A	June 5, 2019	5060407	1560
190605_B	June 5, 2019	5060407	1700

190605_C	June 5, 2019	5060407	1685
190606_A	June 6, 2019	5060380	2270
190606_A	June 6, 2019	5060314	1590
190606_A	June 6, 2019	5060382	1550
190606_A	June 6, 2019	5060407	1530
190607_A	June 7, 2019	5060380	2190
190607_A	June 7, 2019	5060314	1590
190607_A	June 7, 2019	5060382	1545
190607_A	June 7, 2019	5060407	1530
190607_B	June 7, 2019	5060407	1535
190608_A	June 8, 2019	5060380	1980
190608_A	June 8, 2019	5060314	1570
190608_A	June 8, 2019	5060382	1545
190608_B	June 8, 2019	5060382	1565
190608_A	June 8, 2019	5060407	1580
190608_B	June 8, 2019	5060407	1545
190609_A	June 9, 2019	5060382	1650
190609_A	June 9, 2019	5060407	1530
190610_A	June 10, 2019	5060380	1980
190610_A	June 10, 2019	5060314	1570
190610_A	June 10, 2019	5060382	1645
190610_B	June 10, 2019	5060382	1635
190610_C	June 10, 2019	5060382	1615
190610_A	June 10, 2019	5060407	1535
190612_A	June 12, 2019	5060314	1670
190612_B	June 12, 2019	5060314	1660
190613_A	June 13, 2019	5060380	1800
190613_A	June 13, 2019	5060314	1620
190613_B	June 13, 2019	5060314	1610
190614_A	June 14, 2019	5060314	1650
190614_B	June 14, 2019	5060314	1620
190614_C	June 14, 2019	5060314	1640
190614_D	June 14, 2019	5060314	1610
190615_A	June 15, 2019	5060380	1730
190616_A	June 16, 2019	5060380	1750
190617_A	June 17, 2019	5060380	1745
190624_A	June 24, 2019	5060407	1665
190624_B	June 24, 2019	5060407	1610
190625_A	June 25, 2019	5060407	1475
190625_B	June 25, 2019	5060407	1470
190626_A	June 26, 2019	5060407	1470
190627_A	June 27, 2019	5060407	1625

190628_A	June 28, 2019	5060407	1610
190628_B	June 28, 2019	5060407	1605
190629_A	June 29, 2019	5060407	1560
190711_A	July 11, 2019	5060407	1640
190711_B	July 11, 2019	5060407	1575
190712_A	July 12, 2019	5060407	1630
190712_B	July 12, 2019	5060407	1640
190712_C	July 12, 2019	5060407	1630
190712_D	July 12, 2019	5060407	1480

GNSS / IMU Data

A five-minute INS initialization is conducted on the ground, with the aircraft engines running, prior to flight, to establish fine-alignment of the INS. GPS ambiguities are resolved by flying within ten kilometers of the base stations. During the data collection, the operator recorded information on log sheets which includes weather conditions, lidar operation parameters, and flight line statistics. Near the end of the mission, GPS ambiguities were again resolved by flying within ten kilometers of the base stations to aid in post-processing. Data is sent back to the main office for preliminary processing to check overall quality of GPS / INS data and to ensure sufficient overlap between flight lines. Any problematic data may be re-flown immediately as required.

The airborne GPS data was post-processed using Applanix POSPac Mobile Mapping Suite version 8.x. A fixed-bias carrier phase solution was computed in both the forward and reverse chronological directions. Whenever practical, lidar acquisition was limited to periods when the PDOP was less than 4.0. PDOP indicates satellite geometry relating to position. Generally, PDOP's of 4.0 or less result in a good quality solution, however PDOP's between 4.0 and 5.0 can still yield good results most of the time. PDOP's over 6.0 are of questionable results and PDOP's of over 7.0 usually result in a poor solution. Usually as the number of satellites increase the PDOP decreases. Other quality control checks used for the GPS include analyzing the combined separation of the forward and reverse GPS processing from one base station and the results of the combined separation when processed from two different base stations. An analysis of the number of satellites, present during the flight and data collection times, is also performed.

The GPS trajectory was combined with the raw IMU data and post-processed using POSPac Mobile Mapping Suite version 8.x. The SBET and refined attitude data are then utilized in the LMS Post Processor to compute the laser point-positions – the trajectory is combined with the attitude data and laser range measurements to produce the 3-dimensional coordinates of the mass points. Up to four return values are produced within the Optech LMS processor software for each pulse which ensures the greatest chance of ground returns in a heavily forested area.

GPS Controls

Virtual Ground GNSS Base Station(s) were used to control the lidar airborne flight lines. Trimble CenterPoint™ RTX™ correction service is a high-accuracy, satellite-delivered global positioning service. This technology provides high-accuracy GNSS positioning without the use of traditional reference station-based differential RTK infrastructure and delivers very high cm level accuracy. In addition, CORS (Continually Operating Reference Stations) are at times used to further enhance the airborne solution.

Lidar Calibration – see appendix 1 for a more detailed workflow description

Merrick-Surdex JV takes great care to ensure all lidar acquisition missions are carried out in a manner conducive to post-processing an accurate data set. This begins in the flight-planning stage with attention to GPS baseline distances and GPS satellite constellation geometry and outages. Proper AGPS surveying techniques are always followed including pre- and post-mission static initializations. In-air IMU alignments (figure-eights) are performed both before and after on-site collection to ensure proper calibration of the IMU accelerometers and gyros.

A minimum of one cross-flight is planned throughout the project area across all flightlines and over roadways where possible. The cross-flight provides a common control surface used to remove any vertical discrepancies in the lidar data between flightlines. The cross-flight is critical to ensure flightline ties across the project area. The areas of overlap between flightlines are used to boresight (calibrate) the lidar point cloud to achieve proper flightline to flightline alignment in all three axes. This includes adjustment of both IMU and scanner-related variables such as roll, pitch, heading, timing interval (range), and torsion. Each lidar mission flown is accompanied by a hands-on boresight in the office.

After boresighting is complete a detailed statistical report is generated to check relative and absolute accuracies before filtering of lidar begins.

Relative Accuracy – flight line to flight line

The project representative flight line separation raster (below) depicts the vertical separation of flight lines by thematically coloring the separation magnitude on a color ramp based on relative distance.

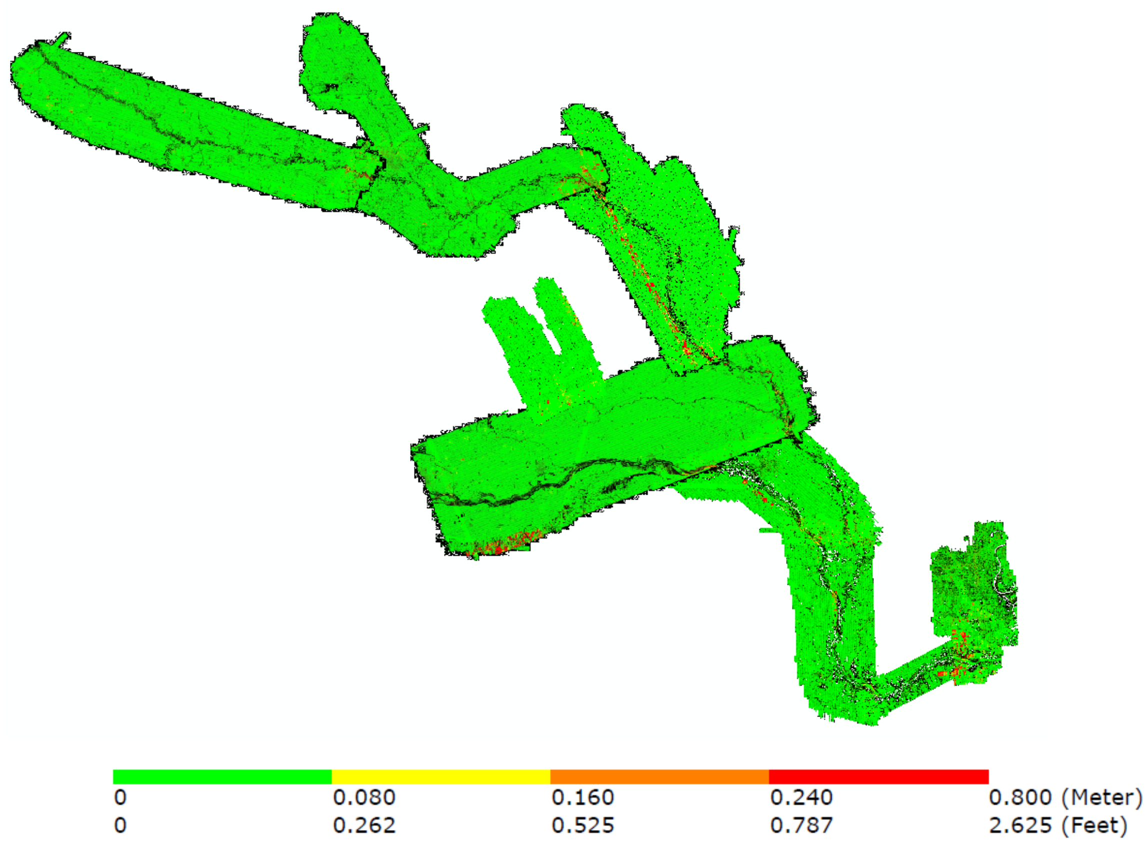

Survey – Lidar Calibration Control / Lidar Checkpoints

CompassData, Inc. surveyors established lidar calibration and lidar checkpoints spatially distributed across the project AOI as the method to validate absolute vertical accuracy. Additionally, photo identifiable (PID) points were collected for use in the aerial triangulation (AT) and horizontal accuracy assessment of the orthoimagery. *See Appendix 2 and 3 for more detailed orthoimagery and survey reporting.*

Unfiltered Lidar Control Point Report

The following tables illustrate the results of the lidar data compared to the lidar control points post-calibration. The listing is sorted by the Z Error column showing, in ascending order, the vertical difference between the lidar points and the forty-two (42) surveyed ground points used for lidar calibration.

Project Data Unit: U.S. Survey Foot
Vertical Accuracy Class tested: 10.0-cm
Elevation Calculation Method: Interpolated from TIN
LiDAR Classifications Included: 2/0 Ground (All)/0W

Check Points in Report: 42
Check Points with LiDAR Coverage: 42
Check Points (NVA): 42
Check Points (VVA): 0
Average Vertical Error Reported: -0.010 U.S. Survey Foot
Maximum (highest) Vertical Error Reported: 0.281 U.S. Survey Foot
Median Vertical Error Reported: 0.006 U.S. Survey Foot
Minimum (lowest) Vertical Error Reported: -0.327 U.S. Survey Foot
Standard deviation of Vertical Error: 0.152 U.S. Survey Foot
Skewness of Vertical Error: -0.505
Kurtosis of Vertical Error: -0.386
Non-vegetated Vertical Accuracy (NVA) RMSE(z): 4.575cm PASS
Non-vegetated Vertical Accuracy (NVA) at the 95% Confidence Level +/-: 8.968cm PASS
FGDC/NSSDA Vertical Accuracy at the 95% Confidence Level +/-: 8.968cm
Non-vegetated Vertical Accuracy (NVA) RMSE(z) (DEM): 4.612cm PASS
Non-vegetated Vertical Accuracy (NVA) at the 95% Confidence Level +/- (DEM): 9.040cm PASS

This data set was tested to meet ASPRS Positional Accuracy Standard for Digital Geospatial Data (2014) for a 10.0-cm RMSEz Vertical Accuracy Class. Actual NVA accuracy was found to be RMSEz = 4.575cm, equating to +/- 8.968cm at the 95% confidence level.

Check Point Id	Check Point X	Check Point Y	Check Point Z	Z from Lidar	Z Error
CAL7038	2729820.844	535517.938	1089.618	1089.291	-0.327
CAL7032	2754747.418	525113.278	1122.997	1122.674	-0.323
CAL7027	2753898.229	494716.676	1081.402	1081.083	-0.319
CAL7001	2657646.379	451832.404	1142.104	1141.854	-0.25
CAL7036	2574873.528	668271.15	1237.104	1236.871	-0.233
CAL7011	2328919.537	576687.592	1492.225	1492.007	-0.218
CAL7046	2195883.149	559614.993	1646.601	1646.39	-0.211
CAL7008	2631243.23	737225.223	1288.384	1288.22	-0.164
CAL7049	2171672.133	1065517.993	1402.953	1402.8	-0.153
CAL7043	2120765.803	524615.061	1723.082	1722.935	-0.147
CAL7028	2102018.297	873720.784	1835.345	1835.273	-0.072
CAL7002	2562888.636	745030.822	1411.96	1411.892	-0.068
CAL7039	2458116.93	704544.354	1459.525	1459.495	-0.03
CAL7048	2002268.239	1082480.874	1582.5	1582.472	-0.028

CAL7050	1882240.603	1101763.469	1695.899	1695.871	-0.028
CAL7003	2375682.995	559071.723	1462.516	1462.489	-0.027
CAL7013	2536050.162	847964.138	1330.943	1330.917	-0.026
CAL7023	2338414.702	806306.794	1523.436	1523.418	-0.018
CAL7035	2572856.206	607829.123	1227.147	1227.133	-0.014
CAL7017	2427006.346	700060.286	1531.982	1531.975	-0.007
CAL7016	2534722.685	795578.017	1458.863	1458.857	-0.006
CAL7015	2366017.422	622336.389	1500.396	1500.413	0.017
CAL7009	2570150.61	827190.789	1336.185	1336.215	0.03
CAL7042	2471519.897	625482.484	1411.444	1411.474	0.03
CAL7005	2633219.776	534844.436	1221.655	1221.693	0.038
CAL7024	2452637.395	889195.875	1441.587	1441.633	0.046
CAL7018	2525820.717	909613.213	1487.868	1487.922	0.054
CAL7020	2424197.219	962245.925	1477.663	1477.724	0.061
CAL7021	2521105.973	643091.826	1361.255	1361.327	0.072
CAL7006	2176836.766	839972.811	1733.709	1733.785	0.076
CAL7025	2117873.091	660165.449	1864.724	1864.8	0.076
CAL7037	2621620.516	557390.683	1282.434	1282.527	0.093
CAL7041	2403252.801	618118.648	1479.739	1479.839	0.1
CAL7026	2310455.883	871684.665	1581.6	1581.721	0.121
CAL7012	2396336.439	780901.984	1453.875	1453.997	0.122
CAL7029	2239426.694	499419.493	1632.549	1632.678	0.129
CAL7030	2436314.317	560736.686	1432.91	1433.066	0.156
CAL7045	2229614.633	814097.31	1675.038	1675.202	0.164
CAL7047	1706703.094	1051413.21	2235.757	2235.937	0.18
CAL7014	2169683.054	600801.086	1715.832	1716.015	0.183
CAL7033	2284823.663	524762.85	1567.806	1568.026	0.22
CAL7007	2641855.453	584140.689	1147.923	1148.204	0.281

Lidar Control Point Layout

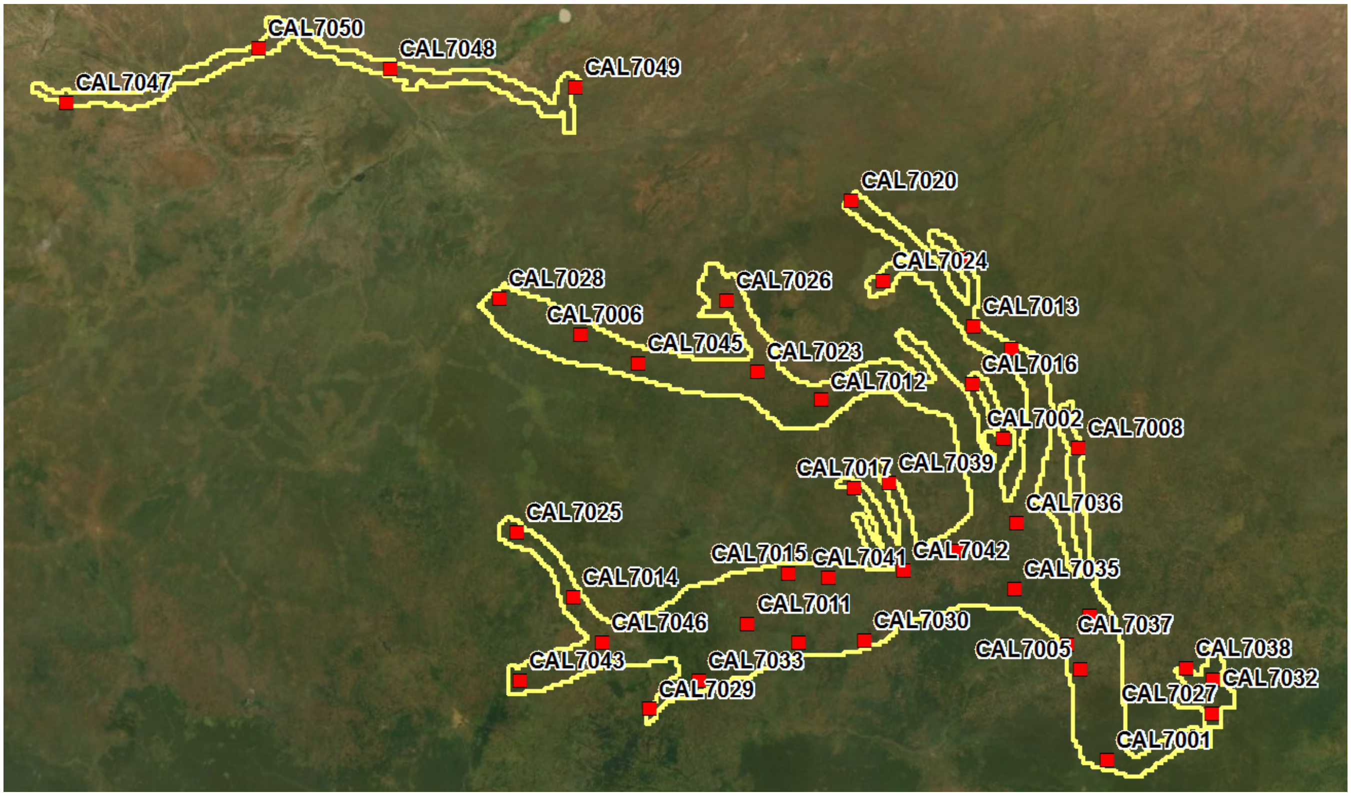

Lidar Filtering and Classification

The lidar filtering process encompasses a series of automated and manual steps to classify the boresighted point cloud data set. Each project represents unique characteristics in terms of cultural features (urbanized vs. rural areas), terrain type and vegetation coverage. These characteristics are thoroughly evaluated at the onset of the project to ensure that the appropriate automated filters are applied and that subsequent manual filtering yields correctly classified data. Data is most often classified by ground and "unclassified", but specific project applications can include a wide variety of classifications including but not limited to buildings, vegetation, power lines, etc. MARS® software is used for the auto-filtering, manual filtering and QC of the classified data.

Merrick-Surdex JV used the ASPRS LAS Specification Version 1.4 – R13, 15 July 2013, Point Data Record Format 6 for this project and classified the lidar point cloud in accordance with the following classification classes and bitflags. The following outlines project specific requirements.

- Class 1 = Unclassified
- Class 2 = Bare-earth Ground
- Class 7 = Low point (noise)
- Class 9 = Water
- Class 17 = Bridge decks
- Class 18 = High noise
- Class 20 = Ignored Ground (breakline proximity)
- Class 21 = Snow (if present and identifiable)

- Class22 = Temporal exclusion (typically non-favored data in intertidal zones)

- Bitflags
    - Withheld: Within the LAS file specification, a single bit flag indicating that the associated lidar point is geometrically anomalous or unreliable and should be ignored for all normal processes.

  Note: Traditional Class 8 (Model Keypoints) points will move to (remain in) Class 2, and will be flagged using the bit flags.

Merrick-Surdex JV has developed several customized automated filters that are applied to the lidar data set based on project specifications, terrain, and vegetation characteristics. A filtering macro, which may contain one or more filtering algorithms, is executed to derive LAS files separated into the different classification groups as defined in the ASPRS classification table. The macros are tested in several portions of the project area to verify the appropriateness of the filters. Often, there is a combination of several filter macros that optimize the filtering based on the unique characteristics of the project. Automatic filtering generally yields a ground surface that is 85-90% valid, so additional editing (hand-filtering) is required to produce a more robust ground surface.

Lidar data is next taken into a graphic environment using MARS® to manually re-classify (or hand-filter) "noise" and other features that may remain in the ground classification after auto filter. A cross-section of the post auto-filtered surface is viewed to assist in the reclassification of non-ground data artifacts. The following is an example of re-classification of the non-ground points (elevated features) that need to be excluded from the true ground surface. Certain features such as berms, hilltops, cliffs and other features may have been aggressively auto-filtered and points will need to be re-classified into the ground classification. Data in the profile view displays non-ground (Unclassified, class 1) in grey and ground in brown/tan (Class 2). In figure 1, a small building was not auto-filtered and needs to be manually re-classified. Note that figure 2 has the building points reclassified to unclassified from the true ground surface.

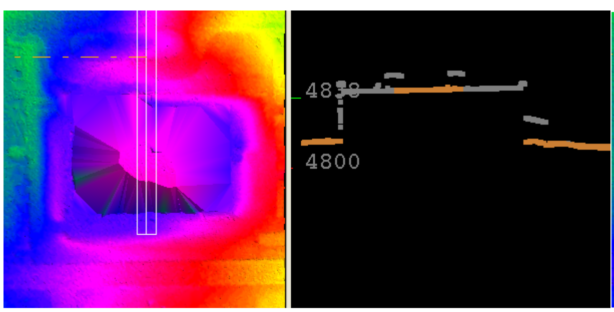

Figure 1

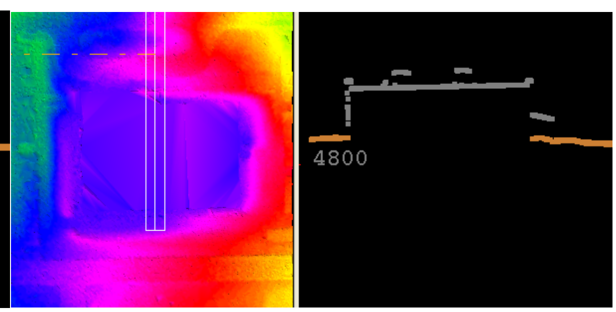

Figure 2

A combination of automated and semi-automated routines to classify buildings and vegetation. We expect that the classified buildings will meet a filtering criterion in the range of 90-95%.

At this point, individual lidar points from the original point cloud have now been parsed into separate classifications.

Filtered Lidar Checkpoint Report

After hand-filtering has been completed and quality checked, a Checkpoint Report is generated to validate that the accuracy of the ground surface is within the defined accuracy specifications. Each surveyed ground check point is compared to the lidar surface by interpolating an elevation from a Triangulated Irregular Network (TIN) of the surface. The MARS® derived report provides an in-depth statistical report, including an RMSE of the vertical errors; a primary component in most accuracy standards and a statistically valid assessment of the overall accuracy of the ground surface.

The below lidar check point report provides statistics for 153 ground survey points used to validate the final filtered lidar surface.

NOTE: despite challenging site conditions, the abovementioned field survey tasks were completed the week of June 17, 2019. The lidar checkpoint and calibration control quantities (and locations) were established prior to the issuance of MODIFICATION P00001; therefore, checkpoint quantities may be out of alignment with the reduction in the DPA.

Units: Meter (/US Survey Feet)

Vertical Accuracy Class tested: 10-cm

Check Points in defined project area (DPA):	153
Check Points with Lidar Coverage	153
Check Points with Lidar Coverage (NVA)	90
Check Points with Lidar Coverage (VVA)	63
Average Z Error (NVA)	0.000/-0.002
Maximum Z Error (NVA)	0.214/0.702
Median Z Error (NVA)	0.003/0.009
Minimum Z Error (NVA)	-0.135/-0.443
Standard deviation of Vertical Error (NVA)	0.053/0.174
Skewness of Vertical Error (NVA)	0.857
Kurtosis of Vertical Error (NVA)	2.583
Non-vegetated Vertical Accuracy (NVA) RMSE(z) [1]	0.053/0.173 PASS
Non-vegetated Vertical Accuracy (NVA) at the 95% Confidence Level +/- [1]	0.104/0.340 PASS
FGDC/NSSDA Vertical Accuracy at the 95% Confidence Level +/-	0.104/0.340
Non-vegetated Vertical Accuracy (NVA) RMSE(z) (DEM) [2]	0.053/0.173 PASS
Non-vegetated Vertical Accuracy (NVA) at the 95% Confidence Level (DEM) +/- [2]	0.103/0.103 PASS
Vegetated Vertical Accuracy (VVA) at the 95th Percentile (DEM) +/- [2]	0.287/0.941 PASS

This data set was tested to meet ASPRS Positional Accuracy Standard for Digital Geospatial Data (2014) for a 10-cm RMSEz Vertical Accuracy Class. Actual NVA accuracy was found to be RMSEz = 5.3cm, equating to +/- 10.4cm at the 95% confidence level. Actual VVA accuracy was found to be +/- 28.7cm at the 95th percentile.

[1] This value is calculated from TIN-based testing of the lidar point cloud data.

[2] This value is calculated from RAM-based grid testing of the lidar data. The grid cells are sized according to the Quality Level selected, and are defined in the USGS NGP Lidar Base Specification Version 1.3 (page 24, Table 6).

Lidar Checkpoint Layout

NVA
VVA

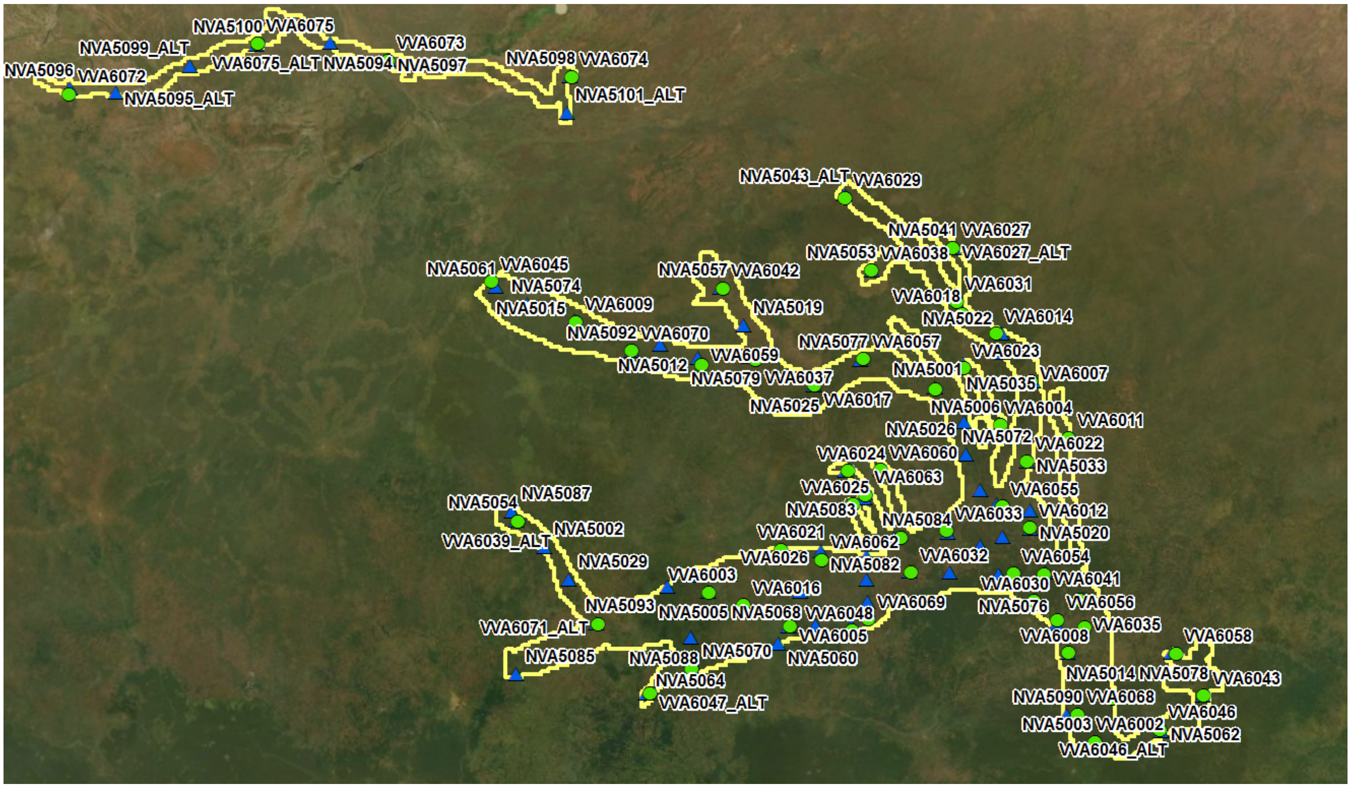

Hydro-flattening Breakline Collection

Hydro- flattening breaklines are captured per the USGS National Geospatial Program Lidar Base Specification Version 1.3. Final hydro-flattened breaklines features are appropriately turned into polygons (flat elevations) and polylines (decreasing by elevation) and are used to reclassify ground points in water to Water (Class 9). The lidar points around the breaklines are reclassified to Ignored Ground (Class 10) based on predetermined buffer.

The next step in the process is the hydro-flattening breakline collection required for the development of the hydro-flattened DEMs. Merrick-Surdex JV will capture hydro-flattening breaklines for waterbodies greater than or equal to two (≥2) acres (~0.8 hectare); double-sided streams and rivers that are greater than or equal to twenty-five feet (≥25'), and; any visible islands greater than or equal to one (≥1) acres (~0.4 hectare). Criteria for Tidal Waters are assumed not applicable. No single-line streams or drainages will be collected, nor will any planimetric features that could be utilized as traditional breaklines. All downstream hydro-flattening breaklines require monotonicity (e.g., streams and rivers). Closed polygonal boundaries of water will maintain a fixed (i.e., flat) elevation. Breaklines are not required to conform to the EleHydro Breakline GIS Data Dictionary for this Task Order.

Linear hydrographic features

To collect hydrographic features, Merrick-Surdex JV uses a methodology that directly interacts with the lidar bare-earth data to collect drainage breaklines. To determine the alignment of a drainageway, the technician first views the area as a TIN of bare-earth points using a color ramp to depict varying elevations. In areas of extremely flat terrain, the technician may need to determine the direction of flow based on measuring lidar bare-earth points at each end of the drain. The operator will then use the color ramped TIN to digitize the drainage in 2D with the elevation being attributed directly from the bare-earth LAS data. MARS® software has the capability of "flipping" views between the elevation TIN, Intensity and imagery, as necessary, to further assist in the determination of the drainage. All drainage breaklines are collected in a downhill direction. For each point collected, the software uses a five-foot (5') search radius to identify the lowest point within that proximity. Within each radius, if a bare-earth point is not found that is lower than the previous point, the elevation for subsequent point remains the same as the previous point. This forces the drain to always flow in a downhill direction. Waterbodies that are embedded along a drainageway are validated to ensure consistency with the downhill direction of flow.

This methodology may differ from those of other vendors in that Merrick-Surdex JV relies on the bare-earth data to attribute breakline elevations. As a result of our methodology, there is no mismatch between lidar bare-earth data and breaklines that might otherwise be collected in stereo 3D as a separate process. This is particularly important in densely vegetated areas where breaklines collected in 3D from imagery will most likely not match (either horizontally or vertically), the more reliable lidar bare-earth data.

Merrick-Surdex JV has the capability of "draping" 2D breaklines to a bare-earth elevation model to attribute the "z" as opposed to the forced downhill attribution methodology described above. However, the problem with this process is the "pooling "effect or depressions along the drainageway caused by a lack of consistent penetration in densely vegetated areas.

Criteria of linear hydrographic breaklines are as follows:

- Linear hydrographic features (e.g., visible streams, rivers, shorelines, canals, etc.) greater than twenty-five feet (25') wide will be captured as a double-lined polygon
    - linear hydrographic features must be flat and level bank-to-bank (perpendicular to the apparent flow centerline) with gradient following the immediately surrounding terrain
    - water surface edge must be at or just below the immediately surrounding terrain
    - streams should break at road crossings (e.g., culverts), and streams and rivers should not break at bridges

Waterbodies

Waterbodies are digitized from the color ramped TIN, similar to the process described above. The elevation attribute is determined as the technician collects the hydro feature by using the lowest bare-earth point within the polygon.

Criteria of waterbody breaklines are as follows:

- Waterbodies (e.g., lakes, ponds, reservoirs) greater than two (2) acres in size are surrounded by a water breakline (i.e., closed polygon)
    - waterbodies must be flat and level with a single elevation for every bank vertex
    - water surface edge must be at or just below the immediately surrounding terrain
    - long impoundments, such as reservoirs or inlets, whose water surface elevations drop when moving downstream should be treated as rivers

Color cycles provide a clear indication of where breaklines are to be collected, especially hydrographic breaklines. Figure 3 demonstrates no breaklines, where Figure 4 is breakline enforced displayed using color cycles within the MARS® software environment.

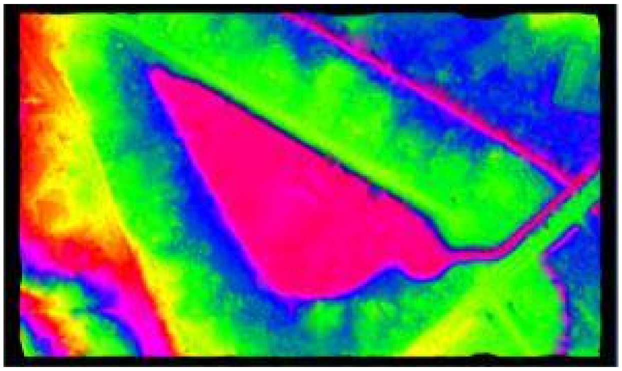

Figure 3

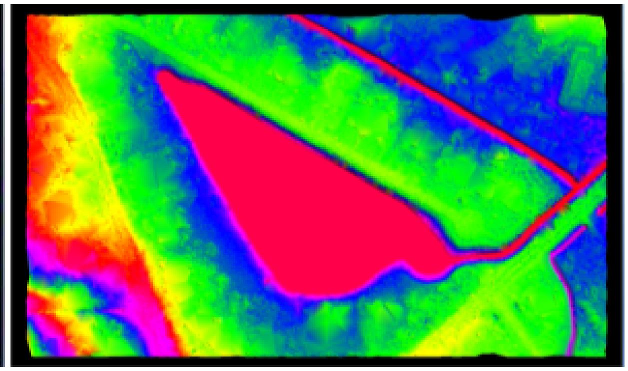

Figure 4

Bare-Earth DEM

Merrick-Surdex JV exports the hydro-flattening breakline enforced Class 2 (ground) lidar points to a one-foot (1ft) cell size, 32-bit format using MARS®, the DEMs are exported to the project tiling scheme. Projection information is applied that reflects the project requirements.

Intensity Images

Merrick-Surdex JV exports all lidar points to a one-foot (1ft) cell size 8-bit client desired format using MARS®, the intensity images are exported to the project tiling scheme and / or project-wide boundary. Projection information is applied that reflects the project requirements.

Contour Generation

Contours are generated using MARS® proprietary software at the desired contour interval. Topology QC checks are completed to ensure topography is logical and complete. Additional QC checks for dangles and appropriate attribution are also verified to comply with project requirements before delivery to the client.

List of Deliverables

- 4-band Ortho Imagery
  - Esri shapefiles
    - Flight lines
    - Tile index
  - 6" pixel resolution 4-band (R,G,B,NIR) 32-bit (8-bit per band) orthoimagery in GeoTIFF format
    - By tile
  - Project-wide compressed ortho imagery in MrSID (Generation 4) format using a 20:1 compression ratio
    - File size dependent
    - Separated products
      - RGB
      - NIR
  - FGDC-compliant metadata
  - Imagery Project Report detailing acquisition, processing, AT and accuracy assessment

- Lidar
  - Minimum standards as outlined in **TM11-B4 / Exhibit 1**
  - Classified lidar point cloud
    - Fully compliant ASPRS LAS 1.4-R13, point record format 6
    - By tile
    - Intensity values normalized (rescaled) to 16-bit
    - FGDC-compliant metadata
  - Bare-earth DEM
    - One-foot (1') cell size 32-bit floating point raster in GeoTIFF (.tif) format
    - Bare-earth (hydro-flattened)
      - Culverts will not be removed from the DEMs
      - Bridges will be removed from the DEMs
    - By tile
    - FGDC-compliant metadata
  - Hydro-flattened breaklines
    - Project-wide Esri feature class(es) for insertion into file geodatabase
      - PolylineZ
      - PolygonZ
    - FGDC-compliant metadata
  - Intensity Images
    - 1' cell size 8-bit, 256 color gray scale in GeoTIFF (.tif) format
    - By tile
    - FGDC-compliant metadata
  - Contours
    - Interpolated at 1' intervals
    - Esri feature class(es) for insertion into file geodatabase
    - By tile
    - FGDC-compliant metadata
  - Control
    - Esri shapefile format
      - NVA, VVA and calibration control
    - FGDC-compliant metadata
  - FGDC-compliant metadata (project level)
  - Detailed Lidar Mapping / Project Report
    - Survey report
  - Miscellaneous
    - Flight Index (feature class / file geodatabase)
    - Raw swath (Esri shapefile)
    - DPA and BPA boundaries (Esri shapefile)
    - 3,000' x 3,000' formatted tiles (Esri shapefile)

Appendix 1

Following is a more detailed lidar calibration workflow description.

LIDAR CALIBRATION AND BLOCK LAS OUTPUT

Note: All figures represented on the following pages are for general illustration purposes, and are not examples derived from the project.

Initial Processing

Lidar data is output as LAS point data using Optech's Lidar Mapping Suite (LMS). LMS matches ground and roof planes plus roof lines to self-calibrate and correct system biases. These biases occur within the hardware of the laser scanning systems, within the Inertial Measurement Unit (IMU) and because of environmental conditions which affect the refraction of light. The systemic biases that are corrected for include scale, roll, pitch, and heading.

In addition to the self-calibration mode LMS runs a "production" mode which applies the self-calibration parameters and then analyzes each individual flight line and applies small adjustments to each line to tie overlapping lidar points even more tightly together.

Boresight Self-Calibration Processing Procedures

An LMS boresight calibration is performed on an as-needed basis to correct scale, roll, pitch and heading biases. A minimum of three overlapping flights are flown in opposing directions with one cross flight.

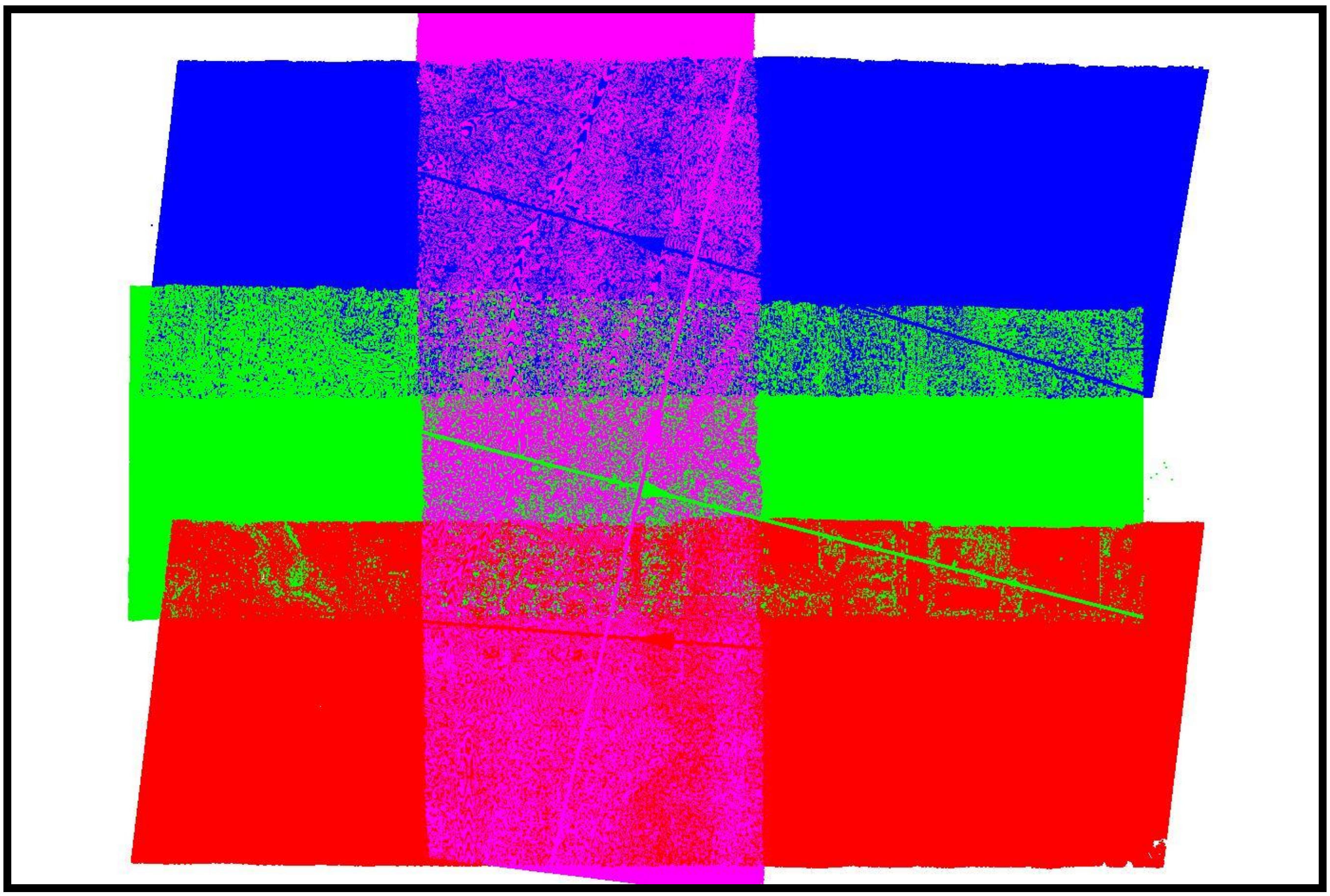

The Boresighting module frees scan angle scale, scan angle lag, XYZ boresight corrections and elevation position corrections while locking scan angle offset and XY position corrections.

The picked calibration site will have a good distribution of buildings for the self-calibration software to match ground planes, roof planes and roof lines.

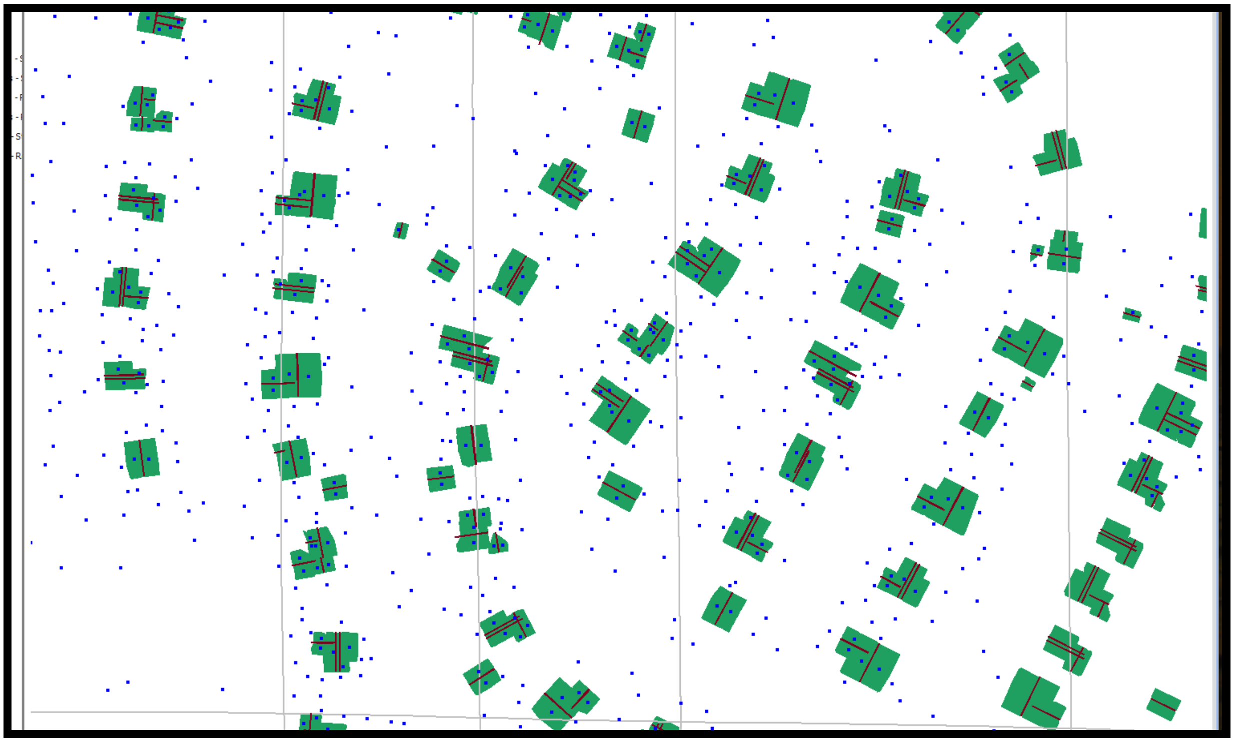

At the conclusion of the self-calibration run the data is quality checked with LMS plots

Plot of plane vertical distances from datum plane.

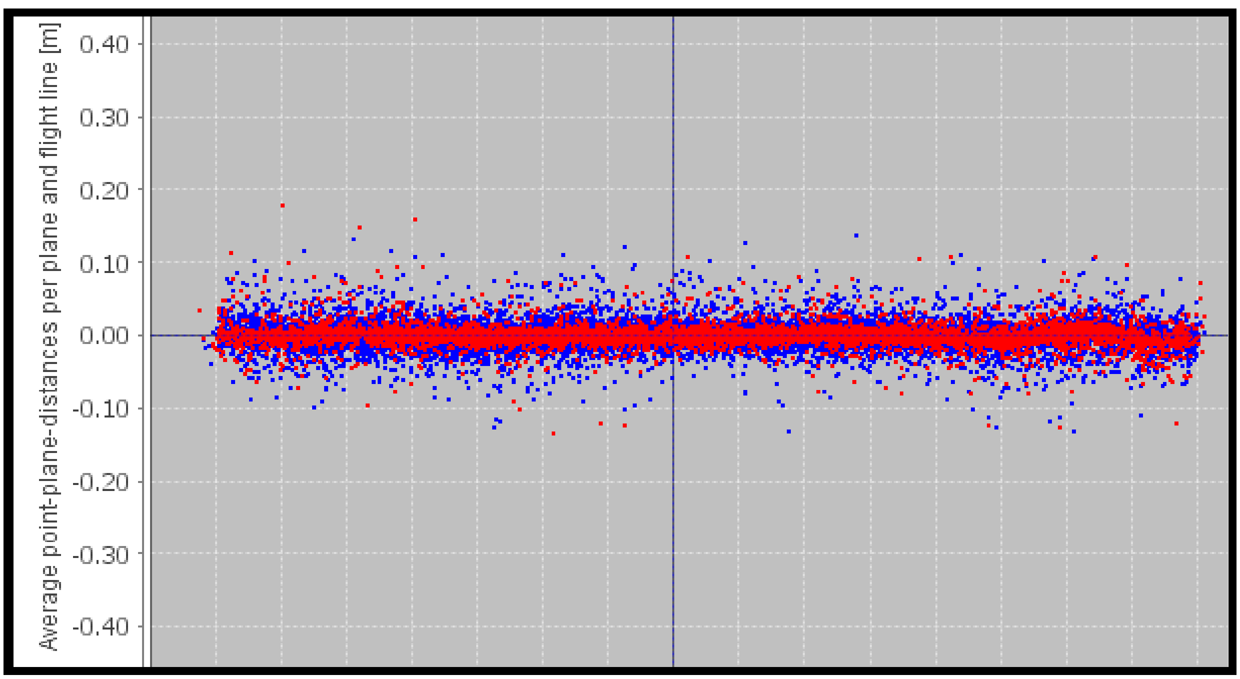

Plot of height differenced between flight lines. (Green=less than 5cm).

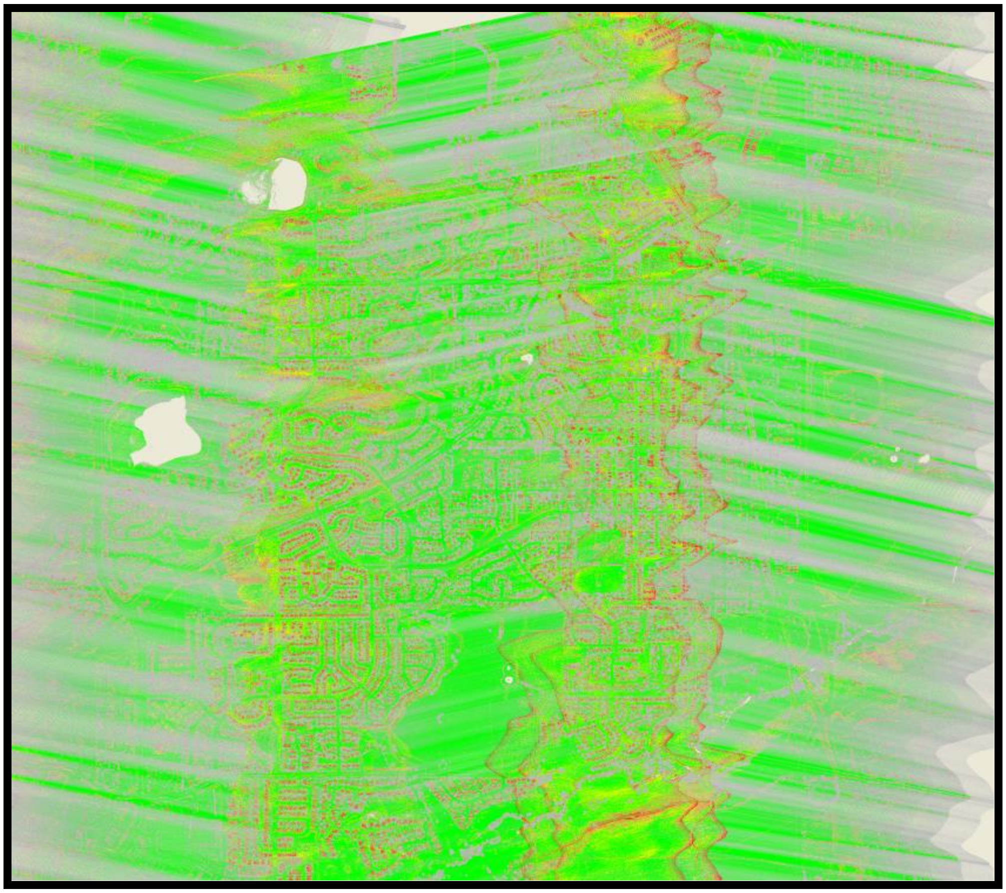

Plot of point densities. (Red=5-9 points per cell, green 10+ points per cell).

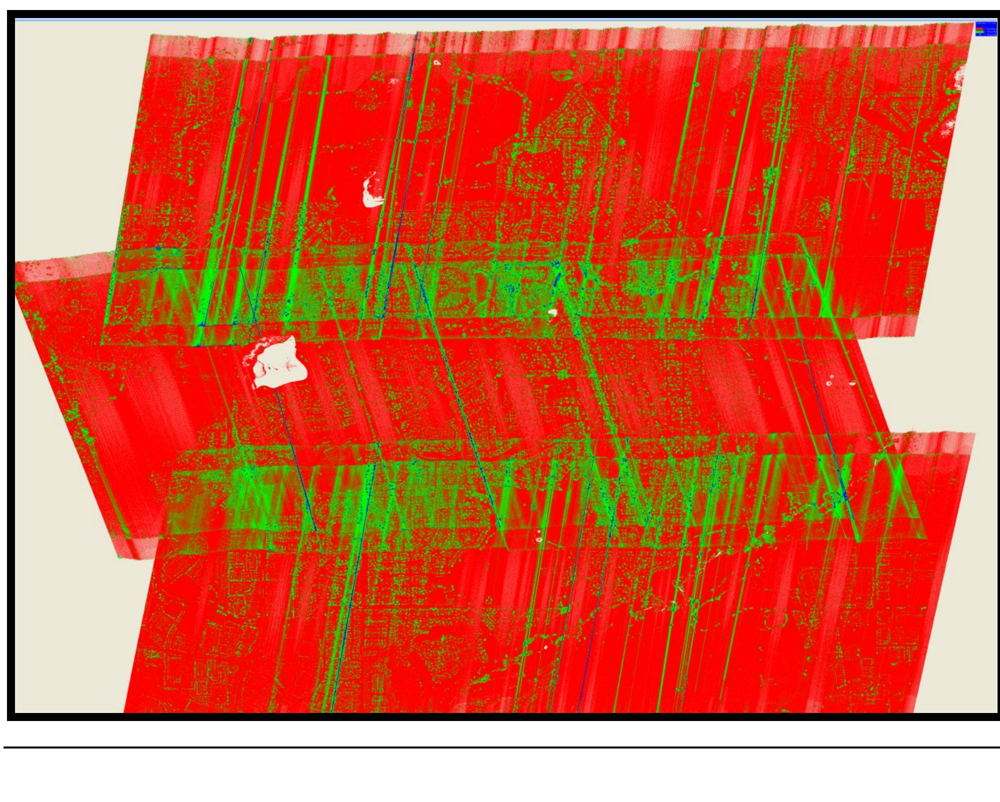

A Flight Line Separation Raster image is generated in Merrick Advanced Remote Sensing Software (MARS®), in this example ground returns from multiple flight lines that are fitting within 3 centimeters are colored green.

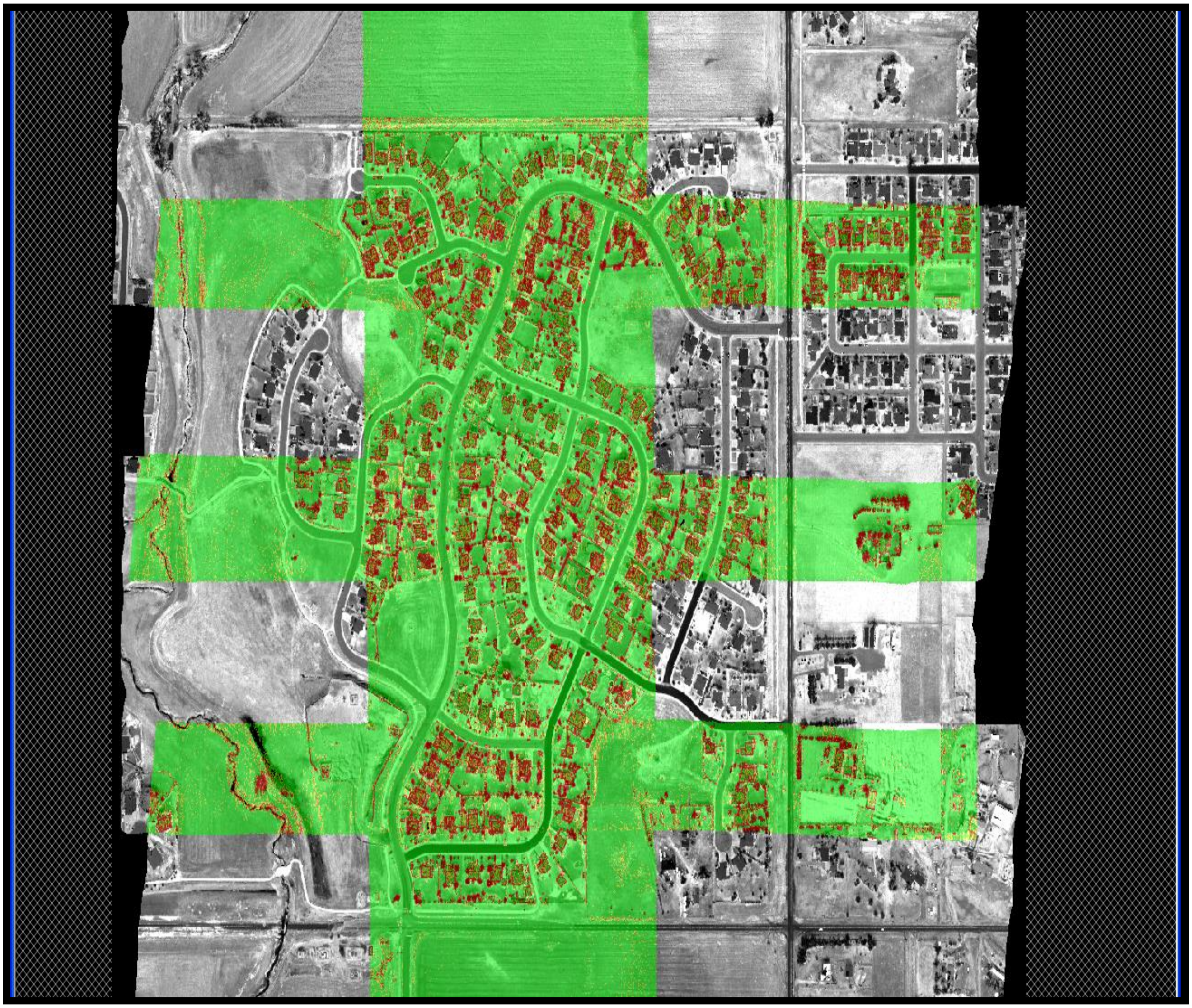

MARS® tests for internal relative vertical accuracy using inbound and outbound scan values. Again, Green is showing inbound and outbound scan data fitting to 3 centimeters.

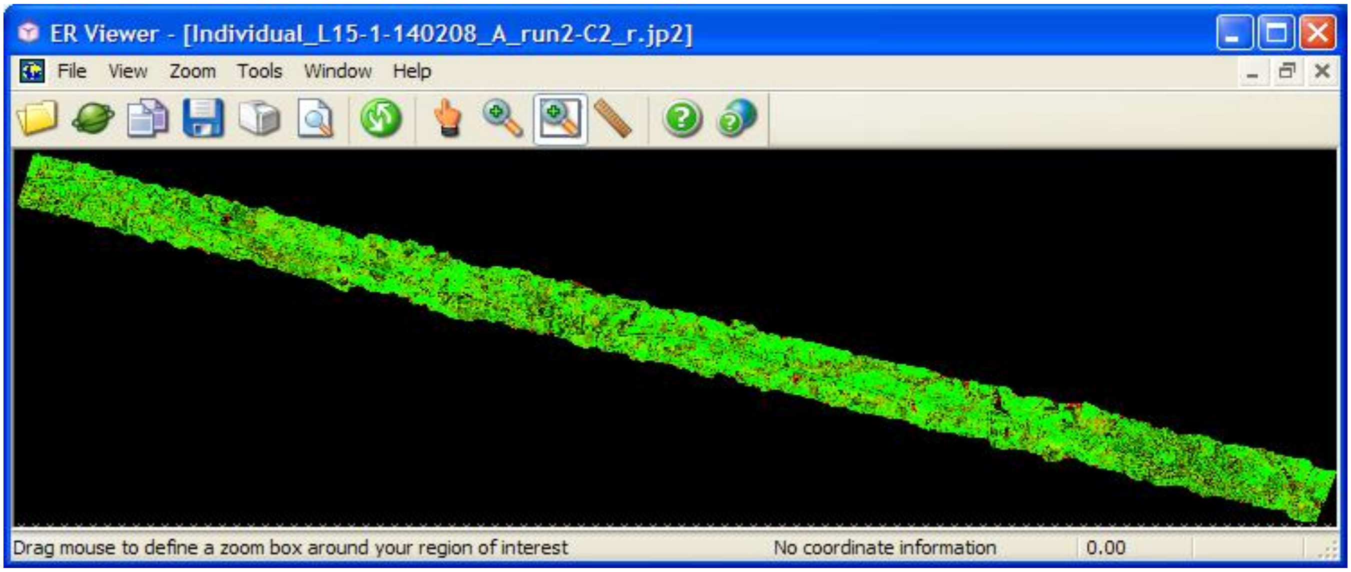

Building cross sections are checked for good alignment. Pitch and heading are checked on roof planes parallel to the flight direction.

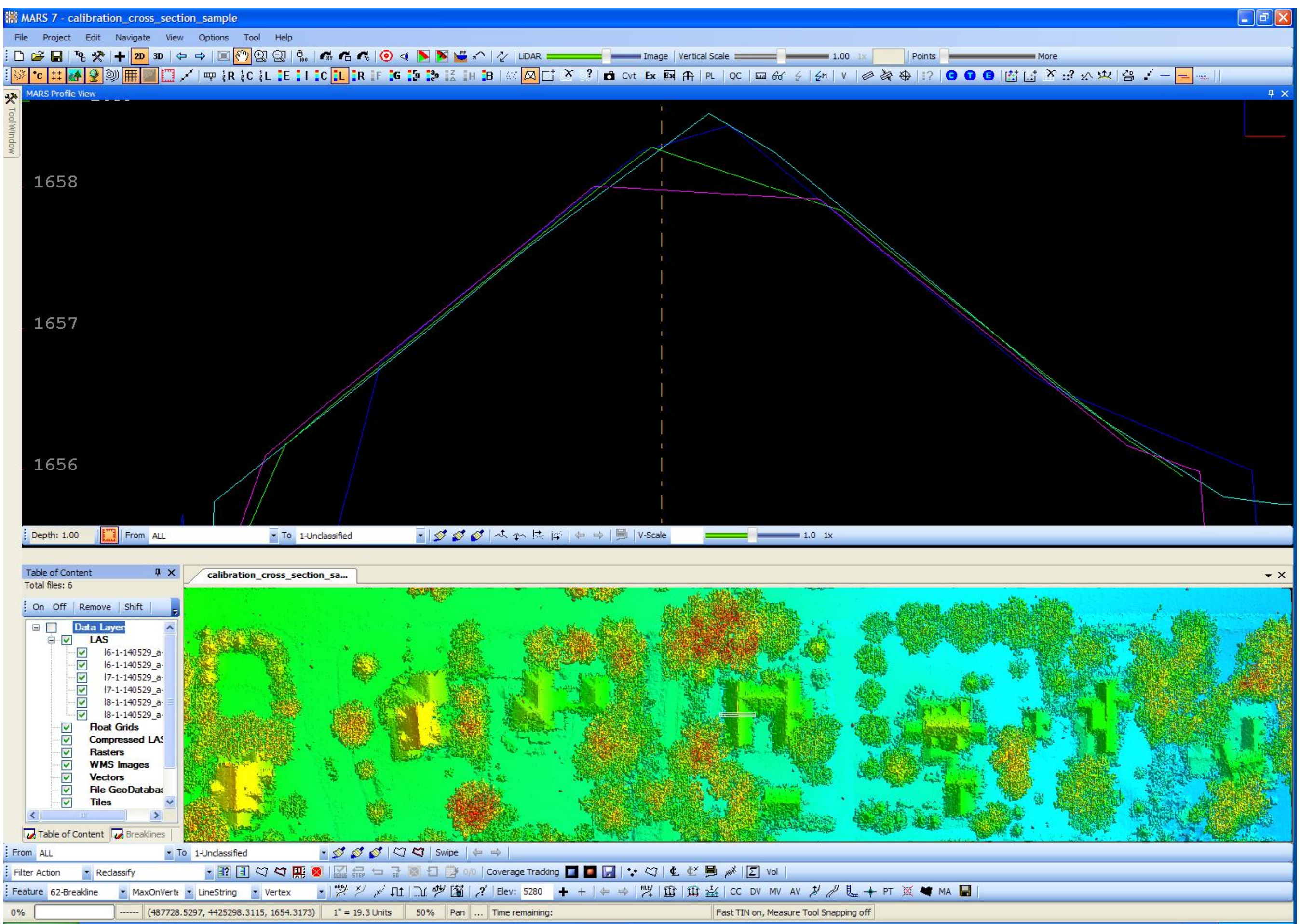

Roll and scale are checked on roof planes perpendicular to the flight direction.

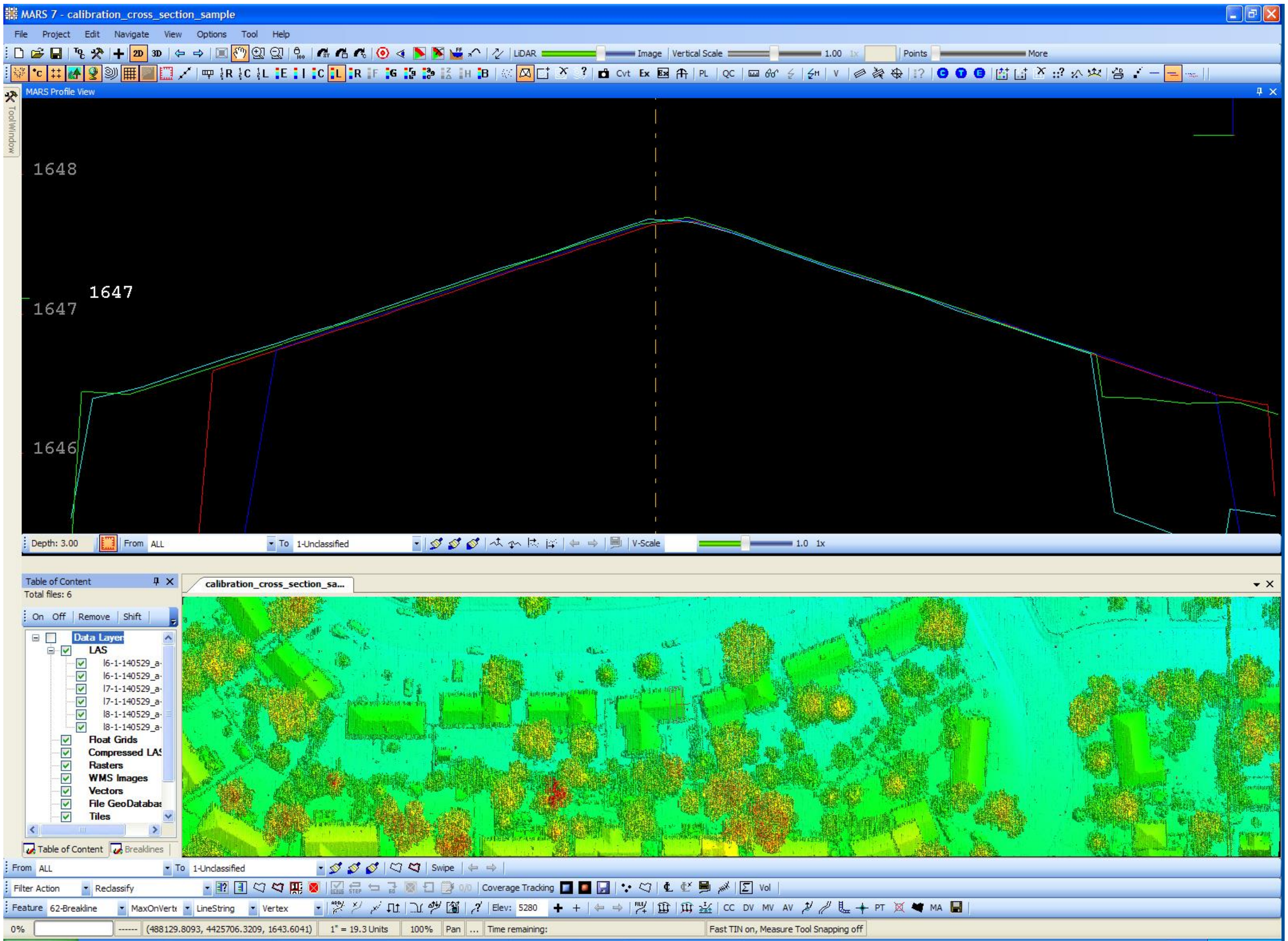

The LMS program outputs a "LCP" file with all the correction parameters. The calibration process may be run several times until the boresight adjustments are acceptable. When the boresight solution is acceptable the LCP file adjustments are saved and also applied to subsequent projects. Each new project is again analyzed and when the adjustment biases show too much drift a new boresight calibration is run. The LCP file may hold calibration tolerances for several projects.

Block LAS Production Processing Procedures

The LMS production mode is run on each flight line to further tie the final lidar LAS flight line files tightly together. Production settings allow scan angle scale, scan angle lag to float and allows elevation to move slightly during flight line to flight line comparison thus further tying flight lines together. A cross flight with locked elevation data is used for controlling flight line elevations.

A block of data is selected to process with LMS production settings. Data collected during turns at the ends of flight lines is deselected (light blue lines).

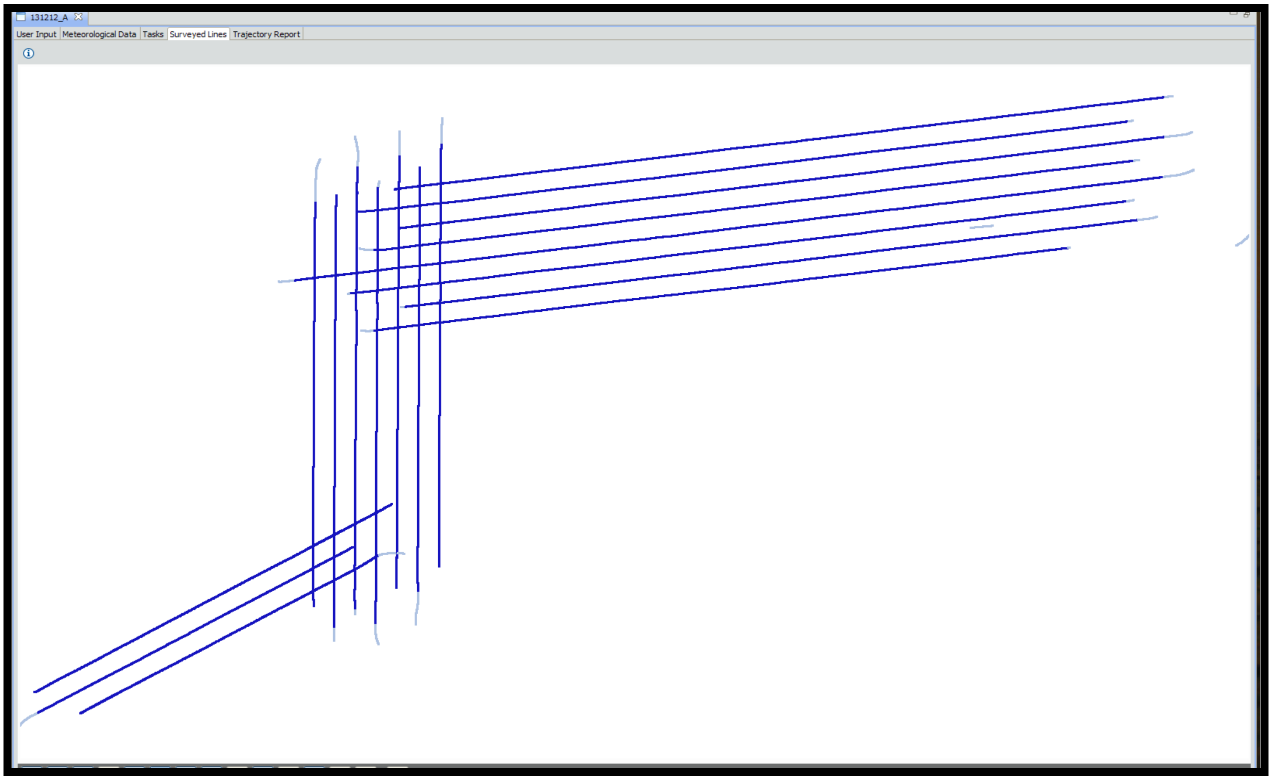

As in self-calibration the LMS production program analyses ground, roof planes and rooflines. One cross flight is locked in elevation and all other lines are adjusted to it. Unlike the calibration site the distribution of roof planes is usually much less dense. Here matched ground tie planes are blue.

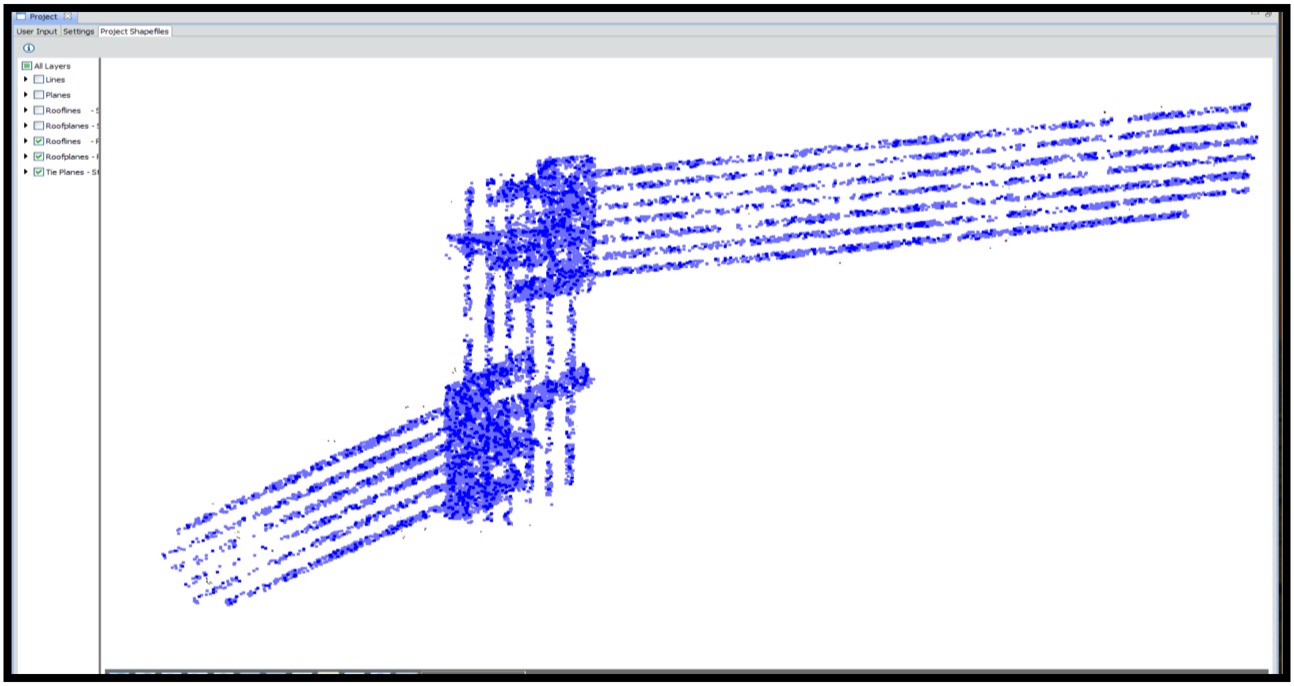

The same quality control outputs used to check self-calibrations are available to analyze the production run. Output plots are again available in LMS and cross sections plus a Flight Line Separation Raster are generated in MARS® to check coverage and quality.

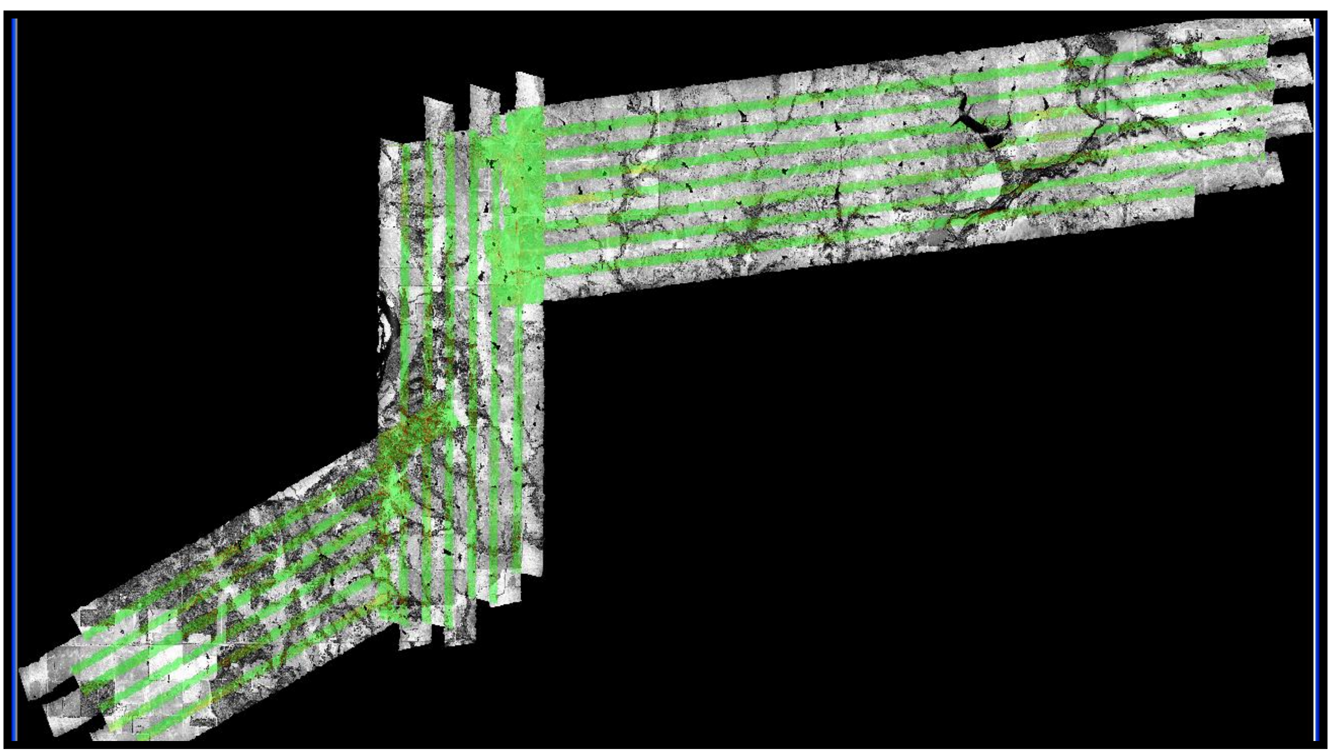

Correcting the Final Elevation

After all the lines are tied together a ground control network is imported into MARS®. The ground control network may be pre-existing or collected by a licensed surveyor.

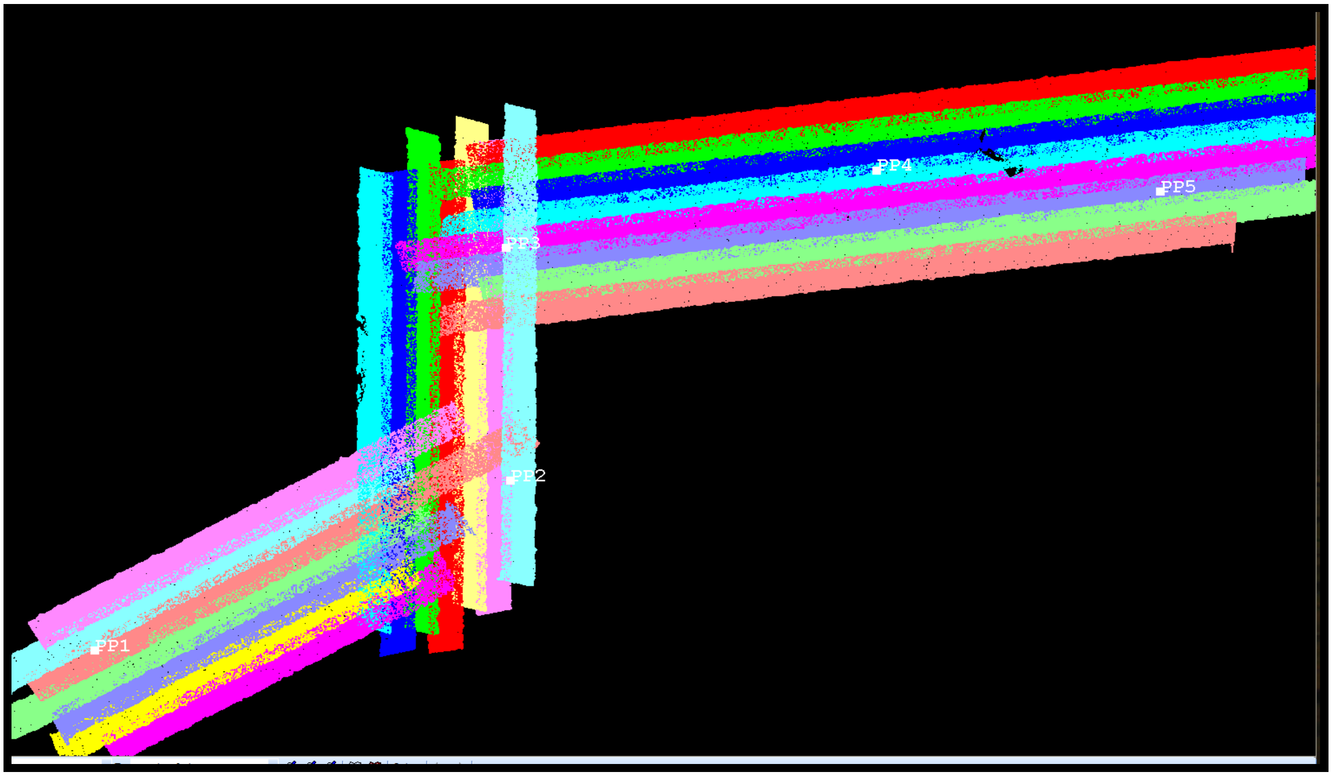

The next step is to match the ground control elevations to the lidar data set. A control report is run and the data set is shifted slightly to zero out the average elevation error and points checked for quality.

The final step before boresighted, leveled LAS files are ready for filtering is to run the MARS® QC Module on the block data. The Boresighted lidar QC Report outputs individual reports on Point Density, Nominal Pulse Spacing, Data Voids, Spatial Distribution, Scan Angles, Control Report, Flight Line Separation, Flight Line Overlap, Buffered Boundary, LAS Formats, Datums and Coordinates.
These reports are checked with the required specifications in the Project Management Plan.

Appendix 2

Following is a more detailed orthoimagery accuracy report.

Aerial Triangulation Report

2019

140G0219F0170-USGS

NE_PostSpringFlood_OrthoLidar_2019_D19 project

Surdex Corporation - Project Number 2900507

August 19, 2019

1.0 Overview

In the Spring of 2019, Surdex performed aerial triangulation on ADS100 imagery collected from multiple Leica ADS100 aerial sensor systems as part of this mapping project for the United States Geological Survey. All aerial imagery was collected with the support of a GNSS/IMU data collection device that collected precision exposure station control and precision angular values. The GNSS/IMU data was post processed with the Novatel Inertial Explorer software to develop precision sensor position and attitude values. All aerial triangulation functions were performed utilizing the latest version of the Leica XPRO software.

ADS 100 camera and accessories (Courtesy of Leica Geosystems).

Pushbroom camera acquisition concept (Courtesy of Leica Geosystems).

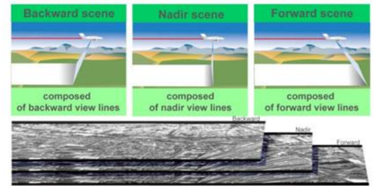

Telecentric lens concept (Courtesy of Leica Geosystems).

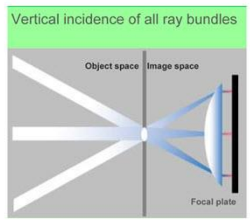

Beam splitting to direct light to separate arrays (Courtesy of Leica Geosystems).

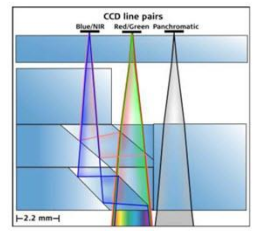

The 6 inch leaf on imagery was flown at approximately 6,100' above mean terrain with flight lines spaced with 30% side overlap. The area encompasses approximately 3,676 square miles in total partially covering 36 counties in Nebraska: Antelope, Boone, Boyd, Brown, Burt, Butler, Cass, Cedar, Colfax, Cuming, Dakota, Dixon, Dodge, Douglas, Greeley, Hamilton, Holt, Howard, Keya Paha, Knox, Madison, Merrick, Nemaha, Otoe, Pierce, Platte, Polk, Richardson, Rock, Sarpy, Saunders, Stanton, Thurston, Washington, & Wayne. The products include 4 band files at 6 inch pixel orthoimagery tiles in TIF fomats. The image below presents the general layout of the leaf on imagery.

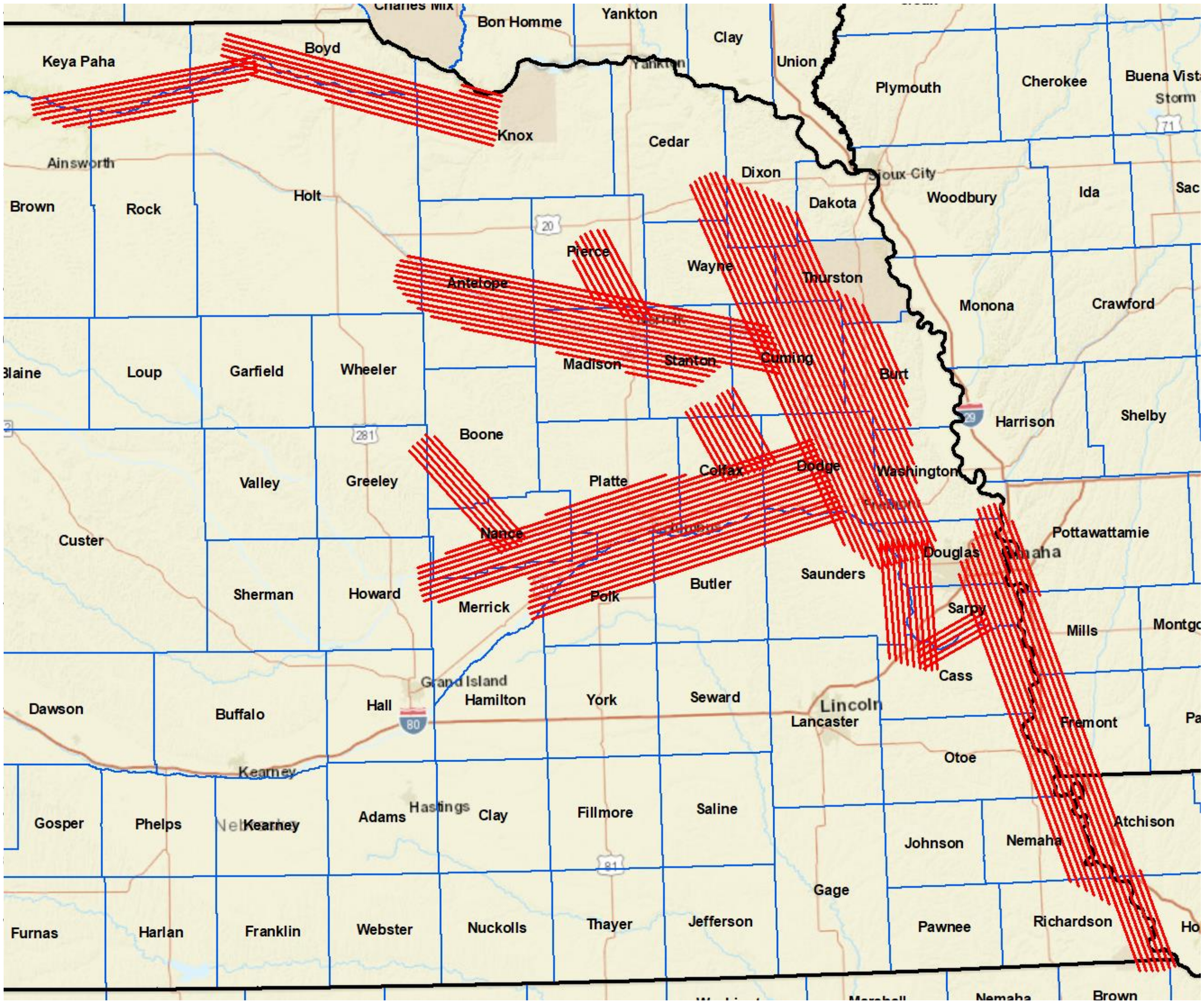

Figure 1: 6-inch ADS100 Flight Lines

2.0 Ground Control

The ground control for the ortho imagery phase of the project consisted of approximately 65 points distributed throughout the area of interest. The ortho control consisted of photo identifiable points. The graphic below represents the layout of the ground control points used for this aerial triangulation. The points were all surveyed by GNSS techniques and processed against NGS monuments in the project area. The final coordinates were derived in NE SPCS (2011) Feet and NAVD88 elevations.

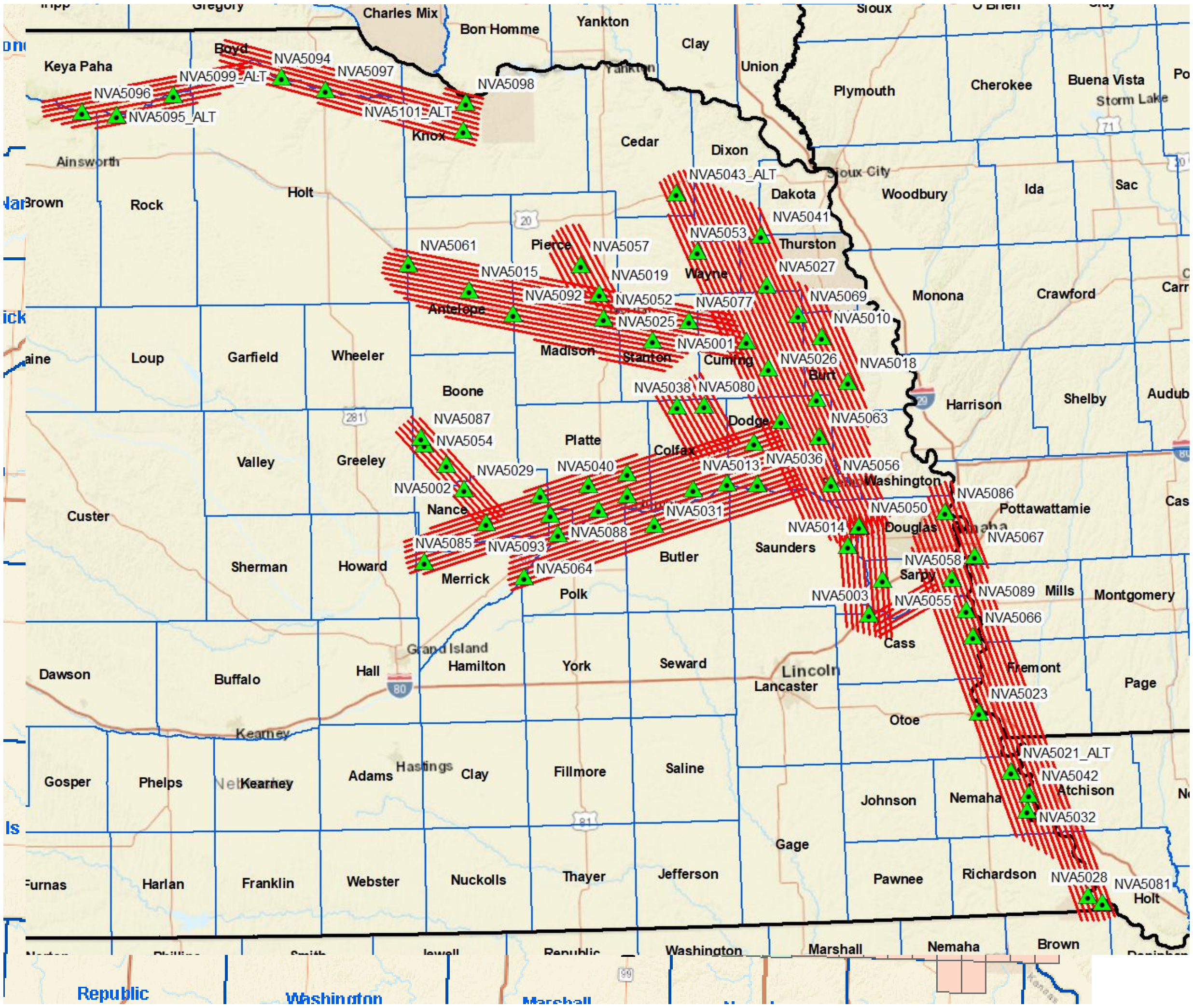

Figure 2: Ground Control Point Distribution

3.0 Aerial Triangulation

Aerial triangulation was performed on the 6-inch imagery as four blocks in the Leica XPro software. The product accuracy requirement of the color digital orthophotography produced under this project is a limiting RMSE in X or Y of 12 inches or less. Based upon these product accuracy standards, we would desire the triangulation results to be under ½ the product horizontal accuracy requirement and equal to the horizontal accuracy requirement of the product in Z (this requirement is derived from section 7.7 of the ASPRS Positional Accuracy Standards for Digital Geospatial Data published in November of 2014). Table 1 below presents the limiting triangulation accuracy values for this project.

Table 1
Triangulation Accuracy Limiting Values

Product Resolution	Product Accuracy RMSE x or y	AT Limiting Accuracy RMSE x or y	AT Limiting Accuracy RMSEz
6-inch	12-inch	6-inch	12-inch

3.1 6-inch Imagery Aerial Triangulation

The required ground control points, images, and GNSS/IMU support data was loaded into XPro. Once in XPro, the block was setup with the appropriate parameters and weights, and initial point measurements were performed. Once completed, the software measured points were run through an ORIMA adjustment. In this adjustment weak and blundered points are automatically removed from the solution. The outcome of this relative adjustment is a set of corrected sensor position and attitude values that accurately model the sensor condition during imagery.

In addition to a textual presentation of the measured points, XPro presents numerous graphical presentations that allow the technicians to refine the triangulation. The graphic below presents several of these graphic displays.

Leica XPro aerial triangulation software interface.

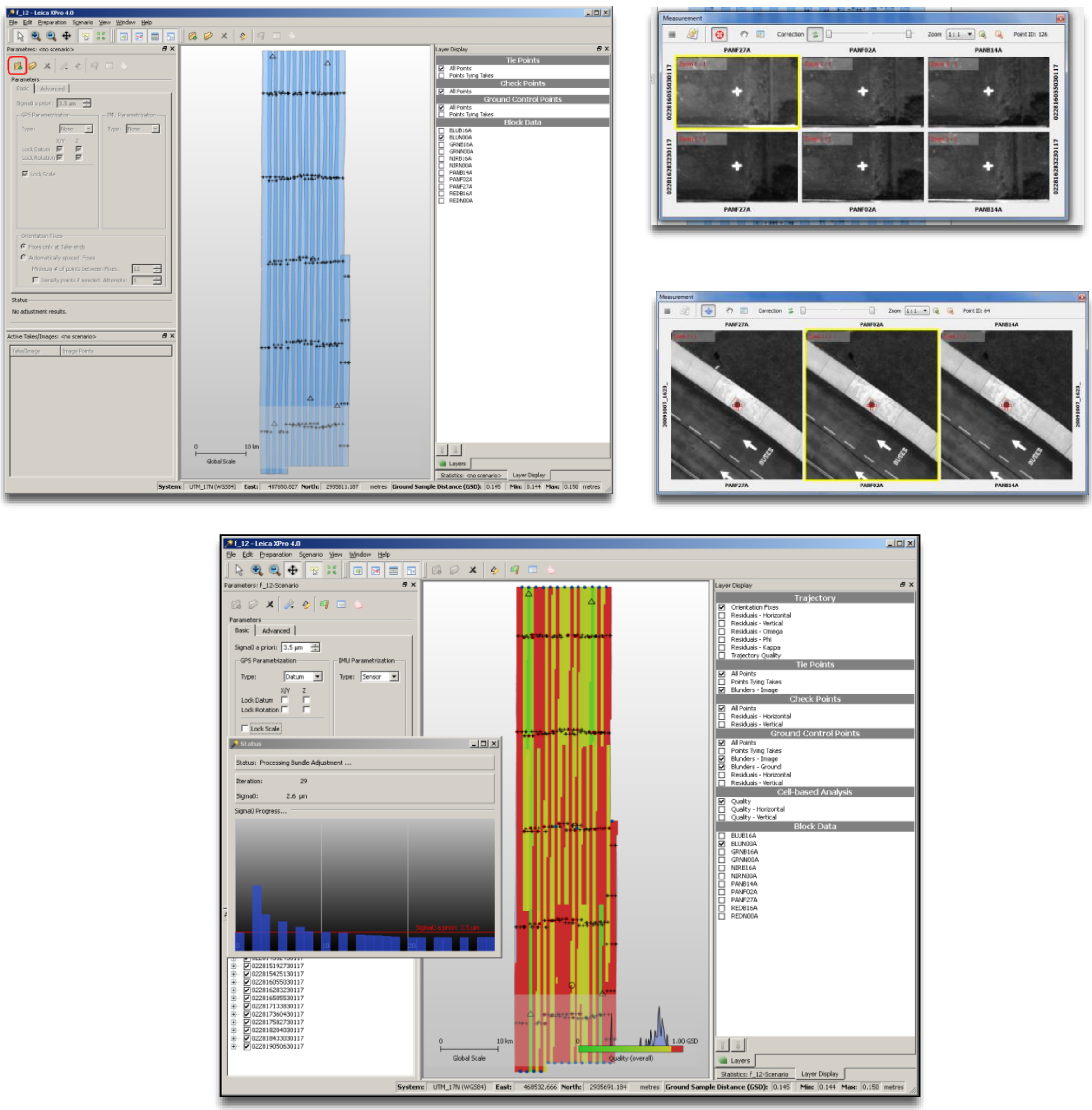

3.1.1 6-inch Final Imagery Aerial Triangulation

The aerial triangulation of this project was completed in four (4) blocks tied together by ground control points. The graphics below presents each block and its corresponding results. The triangulation concept is to assure that the imagery is adjusted to the ground control within the block. By accomplishing this, the final overall aerial triangulation will meet the project accuracy specifications.

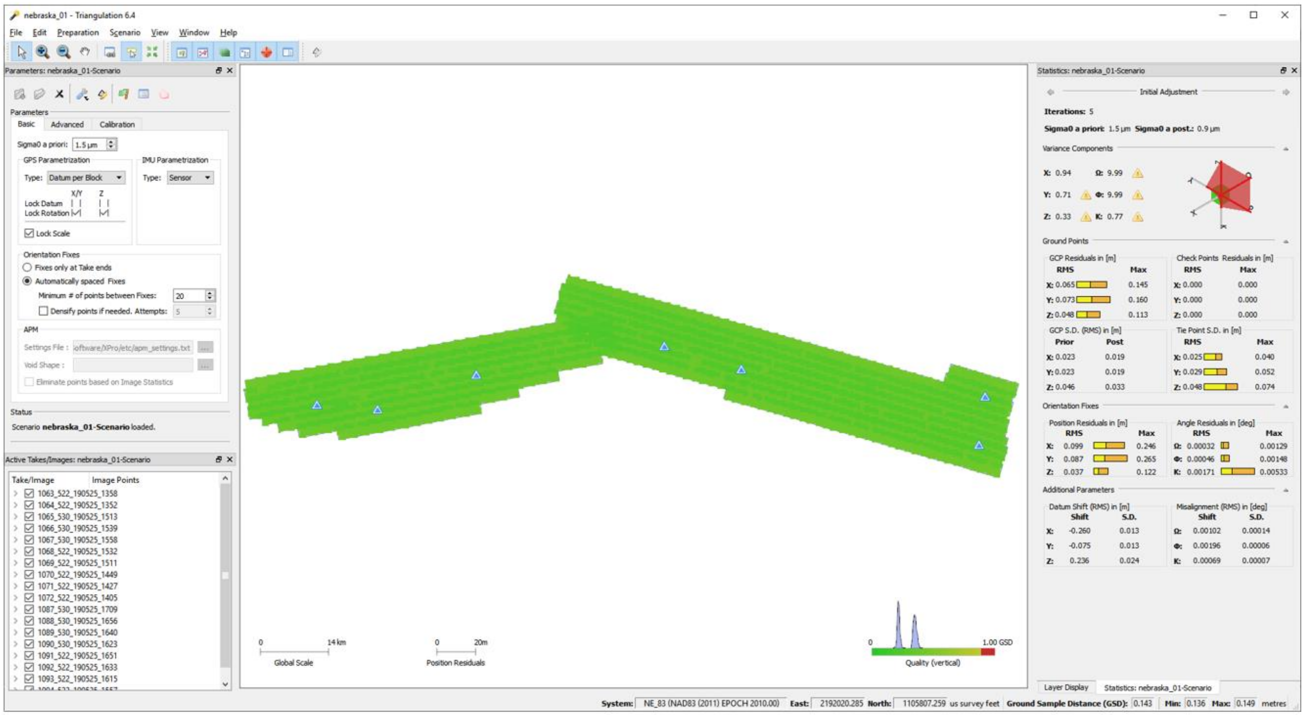

Figure 3: Nebraska Block 1

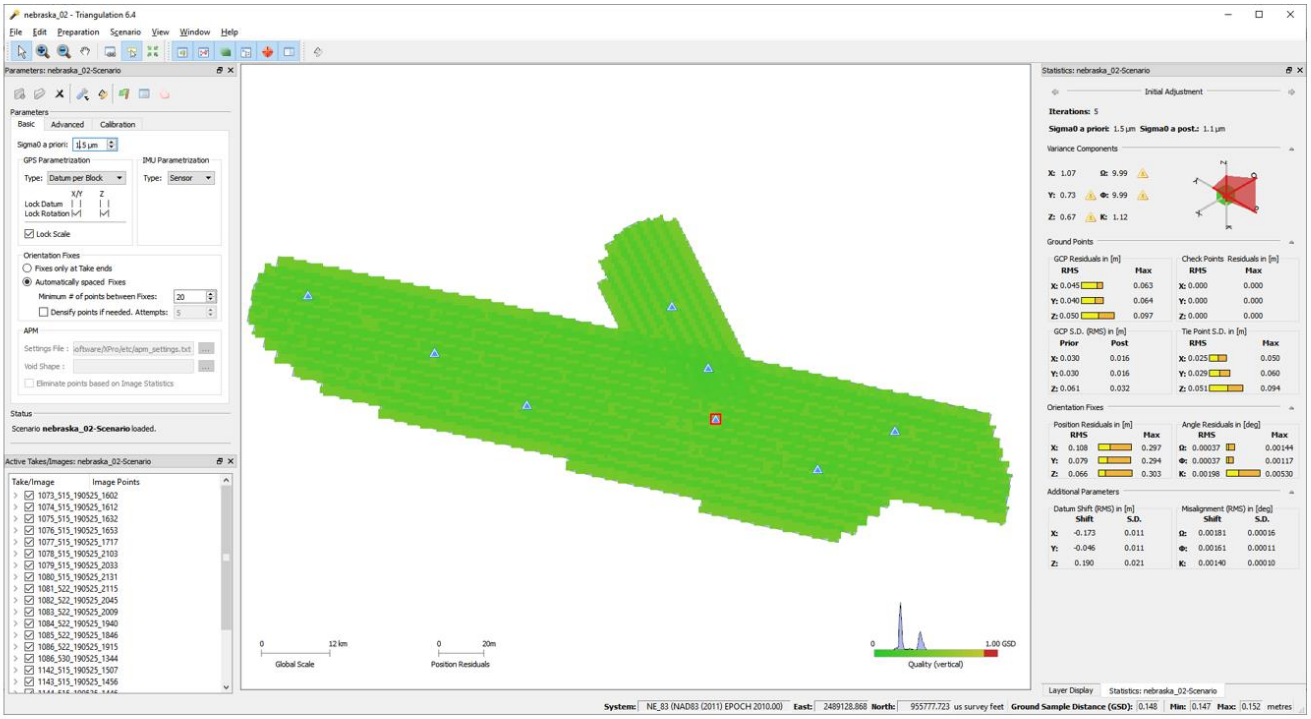

Figure 4: Nebraska Block 2

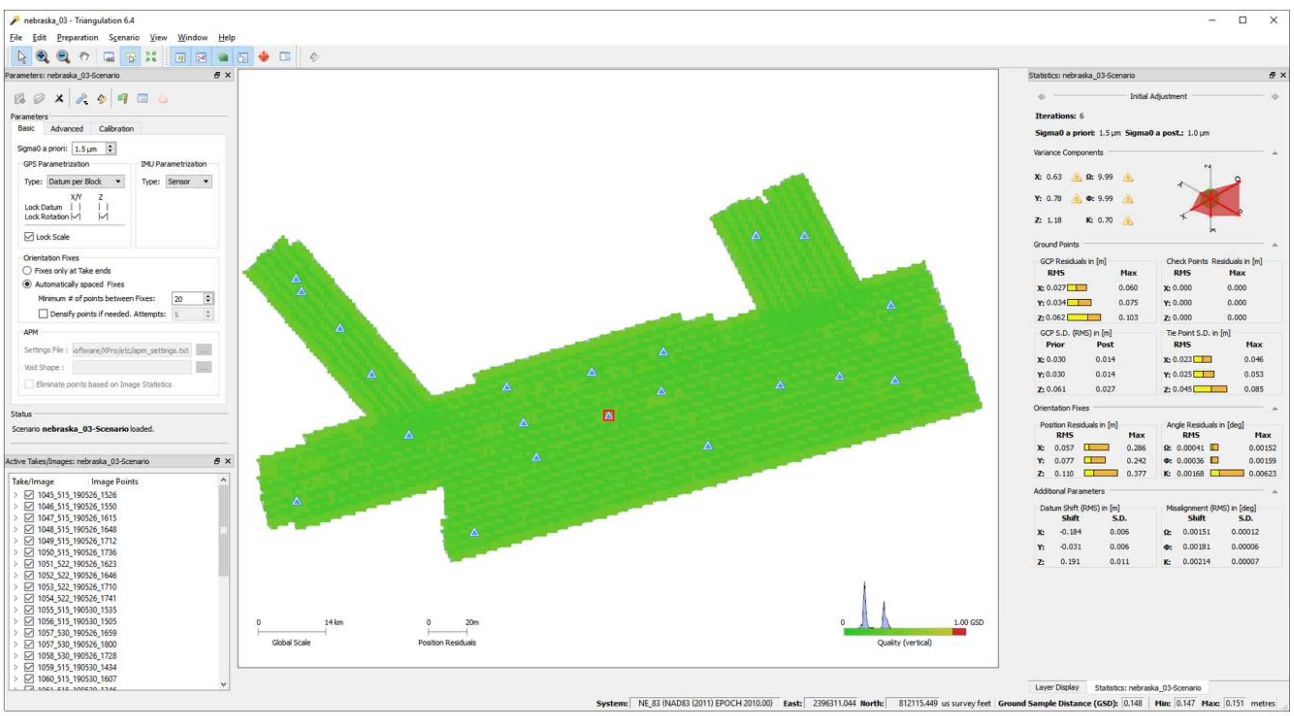

Figure 5: Nebraska Block 3

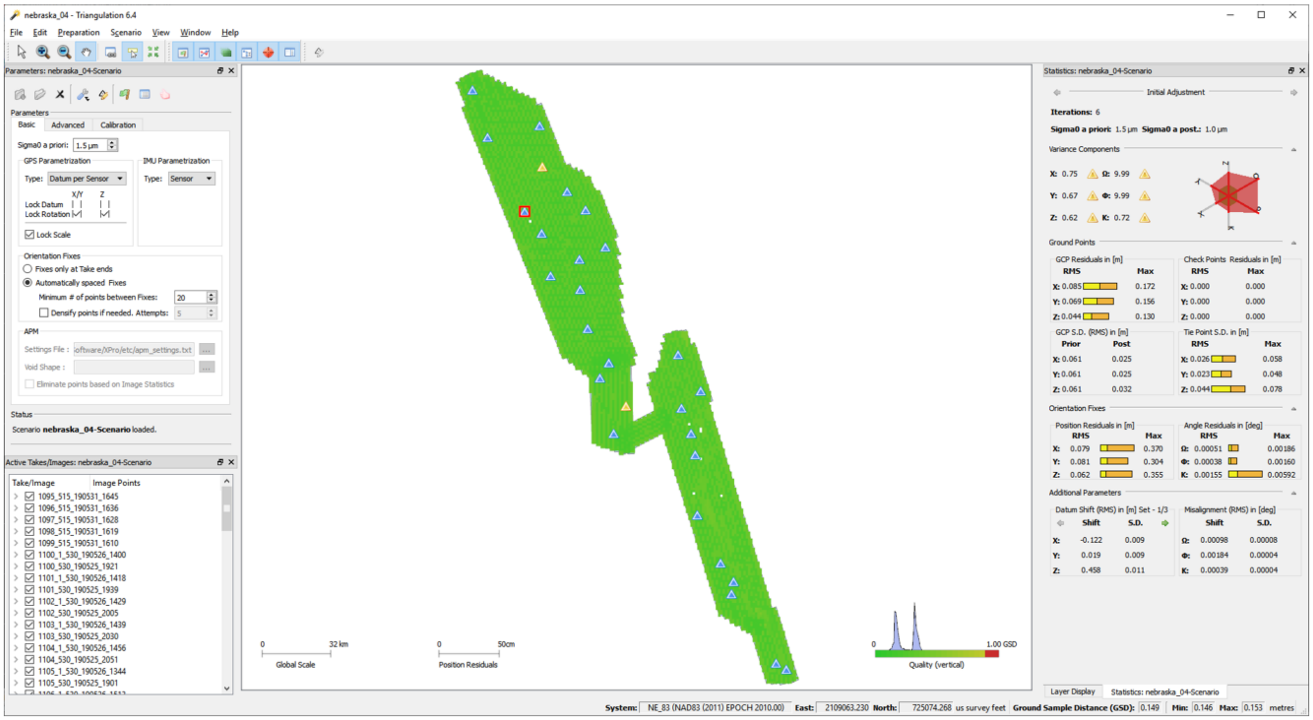

Figure 6: Nebraska Block 4

The key statistics from the aerial triangulation process are summarized in the Table 2 below. All values are meters.

Table 2
Final Aerial Triangulation Statistics

Block ID	Image Residuals (μm)	RMSE Control Points (m)			RMS GNSS Positions (m)			RMS IMU Attitude (deg)		
		δX	δY	δZ	δX	δY	δZ	δΩ	δΦ	δK
Nebraska_1	0.9	0.065	0.073	0.048	0.099	0.087	0.037	0.00032	0.00046	0.00171
Nebraska_2	1.1	0.045	0.040	0.050	0.108	0.079	0.066	0.00037	0.00037	0.00148
Nebraska_3	1.0	0.027	0.034	0.062	0.057	0.077	0.110	0.00041	0.00036	0.00168
Nebraska_4	1.0	0.085	0.069	0.044	0.079	0.081	0.062	0.00051	0.00038	0.00155

The results of Table 2 can be converted to US Survey feet and compared to the project accuracy goals to assess the quality of the triangulation. Tables 3, 4, 5 and 6 below summarize this analysis of the triangulation blocks on this project.

Table 3
Final Triangulation Residuals Summary

Component	Limiting Specification RMSE	Computed RMSE US Survey Foot	Status
X- GCP	0.5-foot	0.21	Passed
Y-GCP	0.5-foot	0.24	Passed
Z-GCP	1.0-foot	0.16	Passed
X-ABGPS	0.5-foot	0.32	Passed
Y-ABGPS	0.5-foot	0.29	Passed
Z-ABGPS	1.0-foot	0.12	Passed

Table 4 Final Triangulation Residuals Summary			
Component	**Limiting Specification RMSE**	**Computed RMSE US Survey Foot**	**Status**
X- GCP	0.5-foot	0.15	Passed
Y-GCP	0.5-foot	0.13	Passed
Z-GCP	1.0-foot	0.16	Passed
X-ABGPS	0.5-foot	0.35	Passed
Y-ABGPS	0.5-foot	0.26	Passed
Z-ABGPS	1.0-foot	0.22	Passed

Table 5 Final Triangulation Residuals Summary			
Component	**Limiting Specification RMSE**	**Computed RMSE US Survey Foot**	**Status**
X- GCP	0.5-foot	0.09	Passed
Y-GCP	0.5-foot	0.11	Passed
Z-GCP	1.0-foot	0.20	Passed
X-ABGPS	0.5-foot	0.19	Passed
Y-ABGPS	0.5-foot	0.25	Passed
Z-ABGPS	1.0-foot	0.36	Passed

Table 6 Final Triangulation Residuals Summary			
Component	**Limiting Specification RMSE**	**Computed RMSE US Survey Foot**	**Status**
X- GCP	0.5-foot	0.28	Passed
Y-GCP	0.5-foot	0.23	Passed
Z-GCP	1.0-foot	0.14	Passed
X-ABGPS	0.5-foot	0.26	Passed
Y-ABGPS	0.5-foot	0.27	Passed
Z-ABGPS	1.0-foot	0.20	Passed

Review of Table 3-6 presents that the aerial triangulations have been performed in a manner that will support further mapping to a limiting RMSE in X and Y of 12-inches or less.

Respectfully submitted,

Steven M. Kasten CP, PLS
August 19, 2019

Appendix 3

Following is a more detailed Survey report.

CompassData
www.compassdatainc.com

Compass Data Inc
7074 S. Revere Parkway
Centennial, Colorado 80112
USA

www.compassdatainc.com
solutions@compassdatainc.com

Project File Data		Coordinate System	
Name:	5932_ NE_PostSpringFlood_v8.vce	Name:	United States/State Plane 1983
Size:	1 MB	Datum:	NAD 1983 (Conus)
Modified:	6/20/2019 9:51:42 AM (UTC:-6)	Zone:	Nebraska 2600
		Geoid:	GEOID12B (Conus)

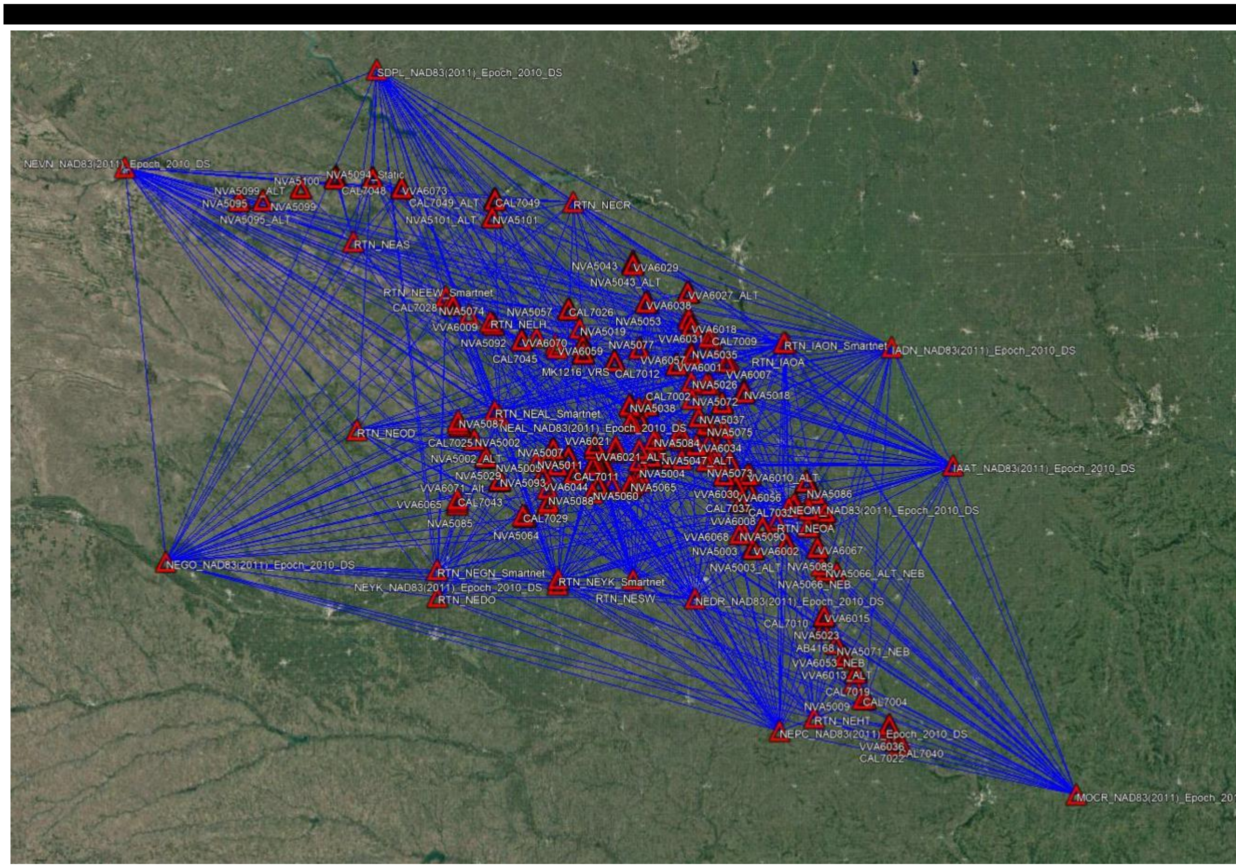

Network Adjustment Report

Adjustment Settings

Set-Up Errors

GNSS

Error in Height of Antenna: 0.003 m

Centering Error: 0.003 m

Covariance Display

Horizontal:

Propagated Linear Error [E]: U.S.

Constant Term [C]: 0.000 m

Scale on Linear Error [S]: 1.960

Three-Dimensional

Propagated Linear Error [E]: U.S.

Constant Term [C]: 0.000 m

Scale on Linear Error [S]: 1.960

Adjustment Statistics

Number of Iterations for Successful Adjustment:	2
Network Reference Factor:	1.01
Chi Square Test (95%):	Passed
Precision Confidence Level:	95%
Degrees of Freedom:	1904

Post Processed Vector Statistics

Reference Factor:	1.00
Redundancy Number:	992.00
A Priori Scalar:	1.06

RTK Vector Statistics

Reference Factor:	1.03
Redundancy Number:	912.00
A Priori Scalar:	0.52

Control Coordinate Comparisons

Values shown are control coordinates minus adjusted coordinates.

Point ID	ΔEasting (Meter)	ΔNorthing (Meter)	ΔHeight (Meter)
NEOM_NAD83(2011)_Epoch_2010_DS	0.003	-0.002	-0.008

Control Point Constraints

Point ID	Type	East σ (Meter)	North σ (Meter)	Height σ (Meter)
IAAT_NAD83(2011)_Epoch_2010_DS	Global	Fixed	Fixed	Fixed
IADN_NAD83(2011)_Epoch_2010_DS	Global	Fixed	Fixed	Fixed
MOCR_NAD83(2011)_Epoch_2010_DS	Global	Fixed	Fixed	Fixed
NEAL_NAD83(2011)_Epoch_2010_DS	Global	Fixed	Fixed	Fixed
NEDR_NAD83(2011)_Epoch_2010_DS	Global	Fixed	Fixed	Fixed
NEGO_NAD83(2011)_Epoch_2010_DS	Global	Fixed	Fixed	Fixed
NELY_NAD83(2011)_Epoch_2010_DS	Global	Fixed	Fixed	Fixed
NEPC_NAD83(2011)_Epoch_2010_DS	Global	Fixed	Fixed	Fixed
NEVN_NAD83(2011)_Epoch_2010_DS	Global	Fixed	Fixed	Fixed
NEYK_NAD83(2011)_Epoch_2010_DS	Global	Fixed	Fixed	Fixed
SDPL_NAD83(2011)_Epoch_2010_DS	Global	Fixed	Fixed	Fixed
Fixed = 0.000001(Meter)				

Adjusted Grid Coordinates

Point ID	Easting Error (Meter)	Northing Error (Meter)	Elevation Error (Meter)
AB4136_SMAR_ATT	0.005	0.006	0.011
AB4136_SMAR_VR	0.005	0.006	0.012
AB4136_VRS_ATT	0.008	0.007	0.015
AB4136_VRS_VR	0.006	0.007	0.012
AB4151	0.006	0.006	0.010
AB4151_rtk	0.006	0.006	0.010
AB4151_Smartnet	0.006	0.006	0.010
AB4168	0.005	0.006	0.012
AB4168_static	0.006	0.006	0.009
CAL7001	0.005	0.006	0.008
CAL7002	0.007	0.010	0.016
CAL7003	0.008	0.012	0.019
CAL7004	0.005	0.005	0.011
CAL7005	0.007	0.008	0.014
CAL7006	0.005	0.005	0.006
CAL7007	0.005	0.006	0.010
CAL7008	0.005	0.005	0.009
CAL7009	0.008	0.008	0.018

CAL7010	0.006	0.007	0.011
CAL7011	0.006	0.006	0.011
CAL7012	0.005	0.006	0.011
CAL7013	0.004	0.005	0.009
CAL7014	0.007	0.006	0.016
CAL7015	0.007	0.007	0.013
CAL7016	0.005	0.006	0.009
CAL7017	0.005	0.006	0.011
CAL7018	0.005	0.006	0.009
CAL7019	0.005	0.006	0.009
CAL7020	0.005	0.006	0.009
CAL7021	0.005	0.005	0.009
CAL7022	0.005	0.007	0.014
CAL7023	0.005	0.006	0.010
CAL7024	0.005	0.005	0.008
CAL7025	0.006	0.007	0.016
CAL7026	0.006	0.008	0.015
CAL7027	0.005	0.005	0.009
CAL7028	0.006	0.007	0.013
CAL7029	0.008	0.013	0.023
CAL7030	0.007	0.010	0.017

CAL7031_IOWA_VRS	0.005	0.005	0.009
CAL7031	0.007	0.006	0.015
CAL7032	0.005	0.005	0.010
CAL7033	0.008	0.009	0.017
CAL7034	0.005	0.005	0.008
CAL7035	0.005	0.006	0.011
CAL7036	0.005	0.006	0.009
CAL7037	0.005	0.005	0.009
CAL7038	0.005	0.006	0.009
CAL7039	0.005	0.005	0.007
CAL7040	0.005	0.006	0.012
CAL7041	0.006	0.006	0.011
CAL7042	0.006	0.007	0.011
CAL7043	0.006	0.007	0.012
CAL7044	0.005	0.006	0.010
CAL7045	0.005	0.005	0.008
CAL7046	0.007	0.007	0.014
CAL7047	0.006	0.007	0.012
CAL7048	0.006	0.007	0.017
CAL7049	0.005	0.005	0.009
CAL7049	0.005	0.006	0.010

CAL7050	0.006	0.007	0.012
hotel001	0.005	0.005	0.007
hotel001_rtk	0.006	0.007	0.012
HOTEL003__Static	0.003	0.003	0.005
HOTEL003_SMART	0.006	0.007	0.012
HOTEL003_VRS	0.006	0.006	0.013
MK1216_SMART	0.005	0.006	0.009
MK1216_SMART_ATT	0.004	0.005	0.008
MK1216_STATIC	0.009	0.010	0.017
MK1216_VRS	0.006	0.008	0.013
MK1216_VRS_ATT	0.005	0.007	0.011
MK2019_SMA_VERIZ	0.008	0.011	0.015
MK2019_SMART_ATT	0.007	0.011	0.010
MK2019_VRS_ATT	0.007	0.008	0.015
MK2019_VRS_VERIZ	0.008	0.010	0.016
NEOM_NAD83(2011)_Epoch_2010_DS	0.002	0.002	0.002
NVA5001	0.005	0.007	0.010
NVA5002	0.006	0.007	0.014
NVA5002_ALT	0.007	0.006	0.017
NVA5003	0.005	0.007	0.010
NVA5003_ALT	0.005	0.006	0.009

NVA5004	0.008	0.011	0.033
NVA5005	0.006	0.007	0.015
NVA5006	0.005	0.006	0.009
NVA5007	0.006	0.006	0.010
NVA5008	0.008	0.013	0.020
NVA5009	0.005	0.005	0.008
NVA5010	0.006	0.008	0.013
NVA5011	0.007	0.006	0.016
NVA5012	0.007	0.008	0.016
NVA5013	0.006	0.006	0.012
NVA5014	0.008	0.011	0.027
NVA5014_ALT	0.006	0.006	0.013
NVA5015	0.004	0.005	0.006
NVA5016	0.005	0.006	0.010
NVA5016_ALT	0.006	0.006	0.010
NVA5017	0.006	0.007	0.014
NVA5018	0.005	0.005	0.009
NVA5018_ALT	0.005	0.007	0.013
NVA5019	0.007	0.008	0.015
NVA5020	0.006	0.007	0.011
NVA5021	0.005	0.006	0.010

NVA5021_ALT	0.005	0.007	0.010
NVA5022	0.006	0.006	0.012
NVA5023	0.007	0.008	0.012
NVA5024	0.005	0.006	0.010
NVA5024_ALT	0.010	0.009	0.023
NVA5024_ALT2_66km_vector	0.005	0.006	0.010
NVA5025	0.005	0.006	0.011
NVA5025_ALT	0.005	0.006	0.010
NVA5026	0.005	0.006	0.012
NVA5027	0.006	0.007	0.017
NVA5028	0.005	0.007	0.013
NVA5029	0.007	0.008	0.020
NVA5029_ALT	0.006	0.006	0.012
NVA5030	0.008	0.008	0.015
NVA5030_ALT	0.005	0.006	0.011
NVA5031	0.007	0.013	0.020
NVA5032	0.005	0.005	0.009
NVA5033	0.007	0.009	0.014
NVA5033_ALT	0.007	0.008	0.015
NVA5034	0.008	0.011	0.014
NVA5035	0.005	0.006	0.010

NVA5036	0.006	0.007	0.014
NVA5037	0.007	0.009	0.017
NVA5037_ALT	0.008	0.008	0.024
NVA5038	0.005	0.006	0.011
NVA5039	0.005	0.006	0.010
NVA5040	0.008	0.009	0.018
NVA5040_ALT	0.007	0.008	0.013
NVA5040_ALT2	0.005	0.006	0.010
NVA5041	0.005	0.006	0.008
NVA5042	0.004	0.005	0.009
NVA5042_ALT	0.005	0.006	0.010
NVA5043	0.005	0.005	0.008
NVA5043_ALT	0.006	0.005	0.009
NVA5044	0.006	0.007	0.014
NVA5045	0.006	0.007	0.015
NVA5046	0.005	0.006	0.011
NVA5047	0.006	0.007	0.012
NVA5047_ALT	0.005	0.007	0.012
NVA5048	0.005	0.006	0.011
NVA5049	0.005	0.006	0.011
NVA5050	0.005	0.005	0.008

NVA5050_ALT	0.005	0.005	0.008
NVA5051	0.005	0.007	0.012
NVA5051_ALT	0.006	0.007	0.013
NVA5052	0.007	0.008	0.016
NVA5053	0.004	0.005	0.007
NVA5054	0.007	0.009	0.019
NVA5055	0.004	0.004	0.006
NVA5056	0.005	0.005	0.010
NVA5057	0.008	0.010	0.022
NVA5058	0.005	0.005	0.010
NVA5059	0.007	0.007	0.020
NVA5060	0.008	0.016	0.020
NVA5061	0.006	0.008	0.013
NVA5061_NOID	0.005	0.006	0.008
NVA5062	0.009	0.010	0.020
NVA5063	0.007	0.008	0.013
NVA5064	0.009	0.011	0.030
NVA5065	0.007	0.011	0.019
NVA5066_ALT	0.005	0.006	0.011
NVA5066_IOWA	0.005	0.005	0.009
NVA5066	0.005	0.005	0.010

NVA5067	0.005	0.005	0.008
NVA5067_ALT	0.005	0.005	0.010
NVA5068	0.007	0.007	0.013
NVA5069	0.006	0.007	0.014
NVA5070	0.008	0.009	0.018
NVA5071	0.006	0.006	0.012
NVA5072	0.006	0.007	0.012
NVA5073	0.006	0.007	0.014
NVA5074	0.005	0.005	0.008
NVA5075	0.005	0.006	0.010
NVA5076	0.006	0.006	0.010
NVA5076_ALT	0.005	0.005	0.009
NVA5077	0.005	0.006	0.011
NVA5078	0.005	0.005	0.008
NVA5079	0.005	0.006	0.008
NVA5080	0.005	0.005	0.008
NVA5081	0.006	0.007	0.015
NVA5081_1	0.007	0.009	0.018
NVA5082	0.008	0.008	0.015
NVA5083	0.005	0.005	0.008
NVA5084	0.007	0.007	0.011

NVA5085	0.007	0.009	0.015
NVA5086	0.005	0.005	0.009
NVA5087	0.006	0.011	0.017
NVA5088	0.006	0.006	0.014
NVA5089	0.005	0.005	0.008
NVA5089_ALT	0.005	0.005	0.008
NVA5090	0.005	0.007	0.011
NVA5091	0.009	0.012	0.022
NVA5092	0.005	0.005	0.008
NVA5093	0.007	0.013	0.016
NVA5094_ALT	0.005	0.005	0.009
NVA5094_RTK_36k_7.2cmV	0.005	0.005	0.010
NVA5094	0.005	0.005	0.007
NVA5095	0.005	0.006	0.011
NVA5095_ALT	0.005	0.007	0.011
NVA5096	0.006	0.008	0.015
NVA5097	0.005	0.006	0.009
NVA5097_ALT	0.006	0.006	0.012
NVA5097_ALT_STAT	0.005	0.005	0.008
NVA5098	0.006	0.007	0.017
NVA5098_static	0.005	0.005	0.006

NVA5099	0.005	0.005	0.009
NVA5099_ALT	0.008	0.008	0.016
NVA5100	0.005	0.006	0.008
NVA5100_ALT	0.006	0.006	0.010
NVA5101	0.009	0.009	0.017
NVA5101_ALT	0.008	0.009	0.016
NVV4ALT_?	0.005	0.006	0.010
RTN_IAOA	0.002	0.002	0.003
RTN_IAON_Smartnet	0.002	0.002	0.002
RTN_NEAL_Smartnet	0.002	0.002	0.003
RTN_NEAS	0.002	0.002	0.003
RTN_NECL_Smartnet	0.002	0.002	0.003
RTN_NECO_Smartnet	0.002	0.002	0.003
RTN_NECR	0.002	0.002	0.003
RTN_NEDO	0.002	0.002	0.003
RTN_NEEW_Smartnet	0.002	0.002	0.002
RTN_NEFM_Smartnet	0.002	0.002	0.003
RTN_NEGN_Smartnet	0.002	0.002	0.003
RTN_NEHT	0.002	0.002	0.003
RTN_NELH	0.002	0.002	0.003
RTN_NENO_Smartnet	0.002	0.002	0.002

RTN_NEOA	0.002	0.002	0.003
RTN_NEOD	0.002	0.002	0.003
RTN_NEPR_Smartnet	0.002	0.002	0.002
RTN_NESW	0.002	0.002	0.003
RTN_NEWE	0.003	0.003	0.004
RTN_NEYK_Smartnet	0.003	0.003	0.003
VVA6001	0.009	0.016	0.026
VVA6001_ALT	0.013	0.017	0.035
VVA6002	0.007	0.014	0.020
VVA6003	0.005	0.007	0.013
VVA6004	0.006	0.008	0.012
VVA6005	0.007	0.011	0.020
VVA6006	0.004	0.004	0.006
VVA6007	0.007	0.010	0.017
VVA6008	0.006	0.006	0.012
VVA6009	0.004	0.004	0.006
VVA6010	0.007	0.009	0.016
VVA6010_ALT	0.005	0.006	0.011
VVA6011	0.005	0.005	0.009
VVA6012	0.006	0.006	0.013
VVA6013	0.006	0.008	0.013

VVA6013_ALT	0.005	0.007	0.011
VVA6014	0.006	0.006	0.013
VVA6015	0.009	0.018	0.033
VVA6016	0.006	0.008	0.013
VVA6017	0.005	0.006	0.012
VVA6018	0.011	0.010	0.033
VVA6019	0.005	0.006	0.013
VVA6020	0.011	0.013	0.029
VVA6021	0.008	0.008	0.022
VVA6021_ALT	0.033	0.012	0.027
VVA6022	0.007	0.009	0.016
VVA6022_ALT	0.006	0.007	0.012
VVA6023	0.005	0.006	0.009
VVA6024	0.007	0.007	0.012
VVA6024_ALT	0.006	0.006	0.011
VVA6025	0.008	0.009	0.016
VVA6025_ALT	0.006	0.006	0.010
VVA6026	0.005	0.006	0.014
VVA6027	0.011	0.016	0.035
VVA6027_ALT	0.005	0.006	0.010
VVA6028	0.005	0.006	0.009

VVA6029	0.005	0.005	0.008
VVA6030	0.005	0.006	0.012
VVA6031	0.005	0.006	0.013
VVA6032	0.005	0.006	0.012
VVA6033	0.005	0.007	0.011
VVA6034	0.007	0.010	0.016
VVA6035	0.005	0.005	0.008
VVA6036	0.008	0.012	0.022
VVA6037	0.006	0.006	0.012
VVA6038	0.006	0.009	0.015
VVA6039_ALT	0.016	0.018	0.035
VVA6040	0.005	0.005	0.008
VVA6041	0.012	0.016	0.037
VVA6041_ALT	0.008	0.011	0.021
VVA6042	0.008	0.010	0.026
VVA6042_alt	0.007	0.008	0.018
VVA6043	0.005	0.005	0.011
VVA6044	0.005	0.006	0.011
VVA6045	0.005	0.007	0.010
VVA6046	0.006	0.006	0.011
VVA6046_ALT	0.009	0.010	0.019

VVA6047	0.008	0.009	0.024
VVA6047_ALT	0.006	0.007	0.018
VVA6048	0.005	0.006	0.010
VVA6049	0.005	0.005	0.010
VVA6050	0.005	0.005	0.009
VVA6050_ALT	0.005	0.005	0.009
VVA6051	0.005	0.006	0.009
VVA6052	0.005	0.006	0.012
VVA6052_ALT	0.005	0.006	0.013
VVA6053	0.006	0.006	0.017
VVA6054	0.007	0.007	0.024
VVA6055	0.007	0.011	0.027
VVA6055_ALT	0.006	0.006	0.014
VVA6056	0.006	0.007	0.011
VVA6057	0.005	0.006	0.011
VVA6058	0.005	0.006	0.010
VVA6059	0.006	0.006	0.009
VVA6060	0.011	0.010	0.020
VVA6061	0.006	0.007	0.014
VVA6062	0.005	0.005	0.010
VVA6063	0.006	0.007	0.012

VVA6063_ALT	0.006	0.006	0.010
VVA6064	0.006	0.006	0.010
VVA6064_ALT	0.006	0.006	0.010
VVA6065	0.005	0.006	0.010
VVA6066	0.006	0.006	0.011
VVA6066_ALT	0.006	0.006	0.011
VVA6067	0.006	0.006	0.011
VVA6068	0.005	0.006	0.008
VVA6069	0.005	0.006	0.009
VVA6070	0.006	0.006	0.010
VVA6071	0.009	0.010	0.031
VVA6071_ALT	0.007	0.014	0.027
VVA6072	0.005	0.007	0.011
VVA6073	0.005	0.006	0.012
VVA6074	0.011	0.016	0.035
VVA6075	0.005	0.005	0.008
VVA6075_ALT	0.005	0.005	0.008

Error Ellipse Components

Point ID	Semi-major axis (Meter)	Semi-minor axis (Meter)	Azimuth
AB4136_SMAR_ATT	0.008	0.007	12°
AB4136_SMAR_VR	0.008	0.007	2°
AB4136_VRS_ATT	0.010	0.008	114°
AB4136_VRS_VR	0.010	0.007	154°
AB4151	0.008	0.007	160°
AB4151_rtk	0.007	0.007	61°
AB4151_Smartnet	0.008	0.007	165°
AB4168	0.008	0.006	161°
AB4168_static	0.008	0.007	148°
CAL7001	0.008	0.006	165°
CAL7002	0.013	0.008	20°
CAL7003	0.015	0.009	166°
CAL7004	0.007	0.006	21°
CAL7005	0.010	0.009	159°
CAL7006	0.006	0.006	140°
CAL7007	0.008	0.006	164°
CAL7008	0.006	0.006	166°
CAL7009	0.011	0.009	20°

CAL7010	0.009	0.007	141°
CAL7011	0.008	0.007	1°
CAL7012	0.007	0.006	158°
CAL7013	0.006	0.005	9°
CAL7014	0.009	0.008	117°
CAL7015	0.009	0.008	28°
CAL7016	0.008	0.007	14°
CAL7017	0.008	0.006	12°
CAL7018	0.007	0.006	9°
CAL7019	0.007	0.006	11°
CAL7020	0.007	0.006	17°
CAL7021	0.007	0.006	157°
CAL7022	0.009	0.007	170°
CAL7023	0.007	0.007	0°
CAL7024	0.007	0.006	179°
CAL7025	0.009	0.008	26°
CAL7026	0.009	0.008	9°
CAL7027	0.006	0.006	155°
CAL7028	0.009	0.007	165°
CAL7029	0.017	0.010	5°
CAL7030	0.013	0.008	159°

CAL7031_IOWA_VRS	0.007	0.006	149°
CAL7031	0.009	0.007	122°
CAL7032	0.007	0.006	174°
CAL7033	0.012	0.009	3°
CAL7034	0.007	0.006	24°
CAL7035	0.007	0.006	4°
CAL7036	0.008	0.007	1°
CAL7037	0.007	0.006	27°
CAL7038	0.007	0.006	3°
CAL7039	0.007	0.006	18°
CAL7040	0.008	0.007	164°
CAL7041	0.009	0.007	137°
CAL7042	0.009	0.007	144°
CAL7043	0.009	0.007	165°
CAL7044	0.007	0.007	7°
CAL7045	0.006	0.006	34°
CAL7046	0.010	0.008	133°
CAL7047	0.009	0.007	169°
CAL7048	0.008	0.007	20°
CAL7049	0.007	0.006	166°
CAL7049	0.008	0.007	161°

CAL7050	0.009	0.007	142°
hotel001	0.006	0.006	133°
hotel001_rtk	0.009	0.007	164°
HOTEL003 _Static	0.004	0.004	43°
HOTEL003_SMART	0.008	0.007	4°
HOTEL003_VRS	0.008	0.007	177°
MK1216_SMART	0.008	0.006	169°
MK1216_SMART_ATT	0.007	0.006	172°
MK1216_STATIC	0.013	0.011	172°
MK1216_VRS	0.010	0.008	174°
MK1216_VRS_ATT	0.009	0.007	175°
MK2019_SMA_VERIZ	0.014	0.009	150°
MK2019_SMART_ATT	0.015	0.007	151°
MK2019_VRS_ATT	0.011	0.007	144°
MK2019_VRS_VERIZ	0.013	0.009	147°
NEOM_NAD83(2011)_Epoch_2010_DS	0.002	0.002	95°
NVA5001	0.008	0.007	177°
NVA5002	0.009	0.007	176°
NVA5002_ALT	0.009	0.008	70°
NVA5003	0.009	0.006	166°
NVA5003_ALT	0.008	0.006	166°

NVA5004	0.014	0.010	173°
NVA5005	0.009	0.007	176°
NVA5006	0.007	0.006	23°
NVA5007	0.008	0.007	20°
NVA5008	0.016	0.010	170°
NVA5009	0.006	0.006	22°
NVA5010	0.010	0.007	15°
NVA5011	0.010	0.007	65°
NVA5012	0.011	0.008	36°
NVA5013	0.008	0.007	148°
NVA5014	0.015	0.008	153°
NVA5014_ALT	0.008	0.007	71°
NVA5015	0.006	0.006	142°
NVA5016	0.007	0.006	15°
NVA5016_ALT	0.008	0.007	172°
NVA5017	0.010	0.007	154°
NVA5018	0.007	0.006	10°
NVA5018_ALT	0.008	0.007	2°
NVA5019	0.010	0.008	19°
NVA5020	0.009	0.008	1°
NVA5021	0.008	0.006	22°

NVA5021_ALT	0.008	0.006	22°
NVA5022	0.008	0.007	7°
NVA5023	0.011	0.007	147°
NVA5024	0.007	0.006	16°
NVA5024_ALT	0.012	0.012	82°
NVA5024_ALT2_66km_vector	0.008	0.006	18°
NVA5025	0.007	0.007	169°
NVA5025_ALT	0.007	0.006	166°
NVA5026	0.008	0.007	176°
NVA5027	0.009	0.007	24°
NVA5028	0.009	0.007	173°
NVA5029	0.010	0.009	165°
NVA5029_ALT	0.007	0.007	25°
NVA5030	0.010	0.009	20°
NVA5030_ALT	0.007	0.006	20°
NVA5031	0.016	0.009	167°
NVA5032	0.007	0.006	15°
NVA5033	0.012	0.008	149°
NVA5033_ALT	0.011	0.008	146°
NVA5034	0.015	0.008	152°
NVA5035	0.008	0.007	14°

NVA5036	0.009	0.007	22°
NVA5037	0.011	0.009	16°
NVA5037_ALT	0.011	0.009	112°
NVA5038	0.007	0.006	14°
NVA5039	0.008	0.006	17°
NVA5040	0.011	0.010	166°
NVA5040_ALT	0.010	0.008	170°
NVA5040_ALT2	0.008	0.006	20°
NVA5041	0.007	0.006	5°
NVA5042	0.006	0.006	11°
NVA5042_ALT	0.008	0.006	12°
NVA5043	0.007	0.006	16°
NVA5043_ALT	0.007	0.007	129°
NVA5044	0.009	0.008	3°
NVA5045	0.009	0.007	19°
NVA5046	0.007	0.007	6°
NVA5047	0.009	0.007	144°
NVA5047_ALT	0.009	0.007	167°
NVA5048	0.007	0.006	167°
NVA5049	0.007	0.007	8°
NVA5050	0.007	0.006	149°

NVA5050_ALT	0.007	0.006	148°
NVA5051	0.009	0.006	170°
NVA5051_ALT	0.009	0.007	172°
NVA5052	0.009	0.008	1°
NVA5053	0.006	0.006	176°
NVA5054	0.012	0.009	18°
NVA5055	0.005	0.005	131°
NVA5056	0.007	0.006	148°
NVA5057	0.013	0.010	18°
NVA5058	0.007	0.006	150°
NVA5059	0.009	0.009	148°
NVA5060	0.019	0.010	179°
NVA5061	0.010	0.007	169°
NVA5061_NOID	0.007	0.006	174°
NVA5062	0.012	0.011	163°
NVA5063	0.011	0.007	136°
NVA5064	0.015	0.011	160°
NVA5065	0.014	0.008	159°
NVA5066_ALT	0.007	0.006	146°
NVA5066_IOWA	0.007	0.006	150°
NVA5066	0.007	0.007	145°

NVA5067	0.007	0.006	22°
NVA5067_ALT	0.007	0.006	17°
NVA5068	0.010	0.008	150°
NVA5069	0.009	0.008	13°
NVA5070	0.011	0.009	4°
NVA5071	0.008	0.007	145°
NVA5072	0.009	0.007	20°
NVA5073	0.009	0.007	12°
NVA5074	0.006	0.006	156°
NVA5075	0.007	0.006	11°
NVA5076	0.007	0.007	152°
NVA5076_ALT	0.007	0.007	151°
NVA5077	0.007	0.007	167°
NVA5078	0.007	0.006	1°
NVA5079	0.008	0.006	146°
NVA5080	0.007	0.006	21°
NVA5081	0.009	0.007	154°
NVA5081_1	0.011	0.008	168°
NVA5082	0.011	0.010	138°
NVA5083	0.007	0.006	23°
NVA5084	0.010	0.007	141°

NVA5085	0.012	0.008	166°
NVA5086	0.007	0.006	16°
NVA5087	0.015	0.007	166°
NVA5088	0.007	0.007	157°
NVA5089	0.006	0.006	89°
NVA5089_ALT	0.006	0.006	101°
NVA5090	0.009	0.007	170°
NVA5091	0.016	0.010	150°
NVA5092	0.007	0.006	42°
NVA5093	0.016	0.008	172°
NVA5094_ALT	0.007	0.006	160°
NVA5094_RTK_36k_7.2cmV	0.007	0.006	169°
NVA5094	0.007	0.006	19°
NVA5095	0.008	0.006	160°
NVA5095_ALT	0.008	0.006	159°
NVA5096	0.011	0.007	160°
NVA5097	0.008	0.006	21°
NVA5097_ALT	0.008	0.007	175°
NVA5097_ALT_STAT	0.007	0.007	8°
NVA5098	0.009	0.008	4°
NVA5098_static	0.006	0.006	163°

NVA5099	0.007	0.007	23°
NVA5099_ALT	0.010	0.010	100°
NVA5100	0.007	0.006	143°
NVA5100_ALT	0.009	0.006	143°
NVA5101	0.012	0.011	169°
NVA5101_ALT	0.011	0.010	177°
NVV4ALT_?	0.007	0.006	7°
RTN_IAOA	0.003	0.003	84°
RTN_IAON_Smartnet	0.002	0.002	82°
RTN_NEAL_Smartnet	0.003	0.003	89°
RTN_NEAS	0.003	0.003	101°
RTN_NECL_Smartnet	0.003	0.003	86°
RTN_NECO_Smartnet	0.003	0.003	87°
RTN_NECR	0.003	0.003	108°
RTN_NEDO	0.003	0.003	73°
RTN_NEEW_Smartnet	0.002	0.002	102°
RTN_NEFM_Smartnet	0.003	0.003	86°
RTN_NEGN_Smartnet	0.003	0.003	79°
RTN_NEHT	0.003	0.003	110°
RTN_NELH	0.003	0.003	97°
RTN_NENO_Smartnet	0.002	0.002	90°

RTN_NEOA	0.003	0.003	90°
RTN_NEOD	0.003	0.003	84°
RTN_NEPR_Smartnet	0.002	0.002	79°
RTN_NESW	0.003	0.003	79°
RTN_NEWE	0.004	0.003	148°
RTN_NEYK_Smartnet	0.003	0.003	84°
VVA6001	0.021	0.011	171°
VVA6001_ALT	0.021	0.015	165°
VVA6002	0.017	0.009	168°
VVA6003	0.008	0.007	2°
VVA6004	0.010	0.007	20°
VVA6005	0.014	0.008	158°
VVA6006	0.005	0.004	45°
VVA6007	0.013	0.008	21°
VVA6008	0.008	0.007	36°
VVA6009	0.006	0.005	148°
VVA6010	0.012	0.008	160°
VVA6010_ALT	0.008	0.006	166°
VVA6011	0.006	0.006	176°
VVA6012	0.008	0.007	173°
VVA6013	0.011	0.007	22°

VVA6013_ALT	0.009	0.006	22°
VVA6014	0.008	0.007	176°
VVA6015	0.023	0.011	168°
VVA6016	0.009	0.007	176°
VVA6017	0.007	0.007	156°
VVA6018	0.013	0.012	105°
VVA6019	0.008	0.007	171°
VVA6020	0.020	0.009	39°
VVA6021	0.011	0.010	102°
VVA6021_ALT	0.042	0.011	106°
VVA6022	0.011	0.009	14°
VVA6022_ALT	0.009	0.007	147°
VVA6023	0.007	0.007	18°
VVA6024	0.009	0.008	163°
VVA6024_ALT	0.008	0.008	161°
VVA6025	0.012	0.009	142°
VVA6025_ALT	0.008	0.007	147°
VVA6026	0.008	0.006	146°
VVA6027	0.020	0.013	17°
VVA6027_ALT	0.007	0.006	26°
VVA6028	0.007	0.006	17°

VVA6029	0.007	0.006	10°
VVA6030	0.007	0.007	161°
VVA6031	0.007	0.006	16°
VVA6032	0.008	0.007	179°
VVA6033	0.008	0.006	167°
VVA6034	0.013	0.008	10°
VVA6035	0.007	0.006	151°
VVA6036	0.016	0.010	172°
VVA6037	0.008	0.007	174°
VVA6038	0.012	0.007	170°
VVA6039_ALT	0.023	0.019	150°
VVA6040	0.006	0.006	158°
VVA6041	0.022	0.011	149°
VVA6041_ALT	0.014	0.010	170°
VVA6042	0.013	0.011	173°
VVA6042_alt	0.010	0.008	155°
VVA6043	0.007	0.006	145°
VVA6044	0.007	0.006	151°
VVA6045	0.009	0.006	175°
VVA6046	0.008	0.007	144°
VVA6046_ALT	0.012	0.011	141°

VVA6047	0.011	0.010	163°
VVA6047_ALT	0.009	0.008	152°
VVA6048	0.008	0.006	17°
VVA6049	0.007	0.007	165°
VVA6050	0.007	0.006	20°
VVA6050_ALT	0.006	0.006	17°
VVA6051	0.007	0.006	20°
VVA6052	0.008	0.006	180°
VVA6052_ALT	0.008	0.007	179°
VVA6053	0.008	0.008	131°
VVA6054	0.010	0.009	133°
VVA6055	0.013	0.009	171°
VVA6055_ALT	0.008	0.007	161°
VVA6056	0.009	0.008	153°
VVA6057	0.007	0.007	177°
VVA6058	0.007	0.006	178°
VVA6059	0.008	0.006	144°
VVA6060	0.018	0.007	133°
VVA6061	0.008	0.007	148°
VVA6062	0.007	0.007	39°
VVA6063	0.009	0.008	3°

VVA6063_ALT	0.007	0.007	6°
VVA6064	0.008	0.006	145°
VVA6064_ALT	0.008	0.006	144°
VVA6065	0.007	0.007	161°
VVA6066	0.008	0.007	27°
VVA6066_ALT	0.008	0.007	24°
VVA6067	0.007	0.007	135°
VVA6068	0.008	0.006	169°
VVA6069	0.007	0.006	16°
VVA6070	0.007	0.007	35°
VVA6071	0.014	0.008	37°
VVA6071_ALT	0.018	0.009	169°
VVA6072	0.008	0.007	178°
VVA6073	0.007	0.007	17°
VVA6074	0.019	0.014	1°
VVA6075	0.007	0.006	140°
VVA6075_ALT	0.007	0.006	141°